An Energy Efficient Narrowband Internet of Things Radio Base Station

KARL MINÖR
MASTER´S THESIS
DEPARTMENT OF ELECTRICAL AND INFORMATION TECHNOLOGY
FACULTY OF ENGINEERING | LTH | LUND UNIVERSITY

An Energy Efficient Narrowband Internet of Things Radio Base Station

Karl Minör
cek11kmi@student.lu.se

Department of Electrical and Information Technology
Lund University

Supervisors:
Aleksei Fedorov, Lund University
Jonas Bengtsson, Ericsson
Ulf Morland, Ericsson

Examiner:
Fredrik Rusek, Lund University

June 11, 2020

Printed in Sweden
Tryckeriet i E-huset, Lund

Abstract

NB-IoT was designed as an add-on to the LTE standard to enable wide area cellular connectivity to low-cost devices to facilitate the rapid growth of the Internet of Things. NB-IoT was found to increase the idle power consumption of the radio unit in an example LTE radio base station by almost 17%, costing the mobile network operator not only money, but also harming the environment through increased CO_2 emissions. The objective of this thesis was to identify the reasons for NB-IoT increasing the power consumption in an LTE network, and discovering new methods aiming to mitigate this.

The power consumption increase was identified to be due to the increased mandatory signaling in NB-IoT conflicting with existing power saving features. A major part of the thesis was spent implementing a new method in an Ericsson baseband unit, which was tested in a lab environment. The method reduced the power consumption increase by 50.2% by muting two antenna ports. A second method was investigated which would use multiple carriers and declaring subframes as invalid to retain capacity while reducing power consumption.

It was found that a combination of the two methods could potentially lower the power consumption increase by NB-IoT by up to 74%, which would save an example network in the USA US$2.5 million a year, and lower emissions by 10.9 kilotons of CO_2. Further work needs to be done in this area to investigate the impact these power saving features would have on connectivity in a live network.

Acknowledgments

I would first like to express my gratitude to my supervisors at Ericsson, Jonas Bengtsson and Ulf Morland, for their invaluable guidance, without which, this thesis would not have been possible. I would also like to pay my special regards to Aleksei Fedorov, my supervisor at Lund University, who guided me through the thesis process.

In addition, I would like to thank Fredrik Nilsson and Jens Kongstad for their help with setting up the lab environment, and Peter Nessrup for providing valuable input. Further, I would also like to acknowledge the entire team, NSV PAC Test 4 at Ericsson in Lund, for supporting me and making me feel welcome, as well as Hans Andersson and my previous team, Radio Design 2 at Ericsson in Lund, for providing me with the opportunity that enabled this thesis.

Finally, I would like to thank my family and friends for their support throughout my years of study and through the process of writing this thesis.

Thank you.
Karl Minör

Popular Science Summary

Making Narrowband Internet of Things Truly Low-Cost

Narrowband Internet of Things (NB-IoT), designed to be rolled out in existing 4G networks to provide low-cost connectivity to low-complexity IoT devices, was found to increase the power consumption of the radio in an empty cell by 17%. This thesis presents two new methods that can decrease the power consumption enough to save an operator up to US$2.5 million a year.

The rapid growth of the IoT created a demand for a technology that could provide cheap connectivity to simple devices, such as parking meters or sensors. NB-IoT was designed to support cheap devices with a long battery life of up to 10 years. However, nothing is perfect. While NB-IoT enables low power consumption in its connected devices, measurements in this thesis show that activating NB-IoT in an Long-Term Evolution (LTE) cell increases the power consumption of the radio unit by up to 17%.

As cellular networks consume over 1% of the total electricity grid supply, with a corresponding climate impact, NB-IoT became an expensive technology. Expensive for operators, as power consumption makes up a major part of their operating expenses, but also expensive for humanity, as an increased power consumption comes with increased carbon dioxide emissions. It was the mission of this thesis to identify why NB-IoT increases the power consumption, and to find methods of lowering this.

Investigating the transmissions from an LTE radio base station found that twice as many symbols were transmitted after NB-IoT was activated. Existing power-saving features rely on micro sleep TX, a function that can cut off the power amplifier when no symbols are transmitted. NB-IoT, with its multiple "always on" signals, lower the frequency of micro sleep TX being able to cut off the power amplifier. This thesis therefore focused on maximizing the opportunities for micro sleep TX to cut off the power amplifier.

As each antenna port requires its own power amplifier, removing NB-IoT signaling from antenna ports proved itself a promising concept for lowering the power consumption. A promising method was found, where NB-IoT signals are removed from two antenna ports.

With access to a radio base station, it was possible to implement this solution

into a modified version of the source code. The feature was then verified to be functional in a lab environment with a real device connected to the radio.

Access to a radio base station also allowed accurate power measurements of the new feature. These measurements showed that it was possible to remove half of the power consumption increase. Combining this feature with a novel, unimplemented, feature that changes the placement of NB-IoT signals allows a saving of almost 75%.

Table of Contents

List of Figures

List of Tables

List of Abbreviations

1G	First Generation
2G	Second Generation
3G	Third Generation
3GPP	3rd Generation Partnership Project
4G	Fourth Generation
5G	Fifth Generation
ARQ	Automatic Repeat reQuest
BER	Bit Error Ratio
CIoT	Cellular IoT
CO_2	Carbon Dioxide
CRS	Cell Specific Reference Signal
CSM	Cell Sleep Mode
DCI	Downlink Control Information
DL	Downlink
DSD	Downlink Subframe Deactivation
DU	Digital Unit
eMBB	Enhanced Mobile Broadband
EVM	Error Vector Magnitude
FDD	Frequency-Division Duplex
fm	Frequency Modulation
GSM	Global System for Mobile Communications
ICT	Information and Communications Technology
IoT	Internet of Things
ISI	Intersymbol Interference
LESS	Low Energy Scheduler Solution

LPWAN	Low-Power Wide Area Networks
LTE	Long-Term Evolution
LTE-M	LTE-Machine Type Communication
MCL	Maximum Coupling Loss
MIB-NB	Master Information Block - Narrowband
MIMO	Multiple-Input Multiple-Output
MISO	Multiple-Input Single-Output
mMSM	Massive MIMO Sleep Mode
mMTC	Massive Machine Type Communication
MNO	Mobile Network Operator
MSM	MIMO Sleep Mode
MSTX	Micro Sleep TX
NB	Narrowband
NB-IoT	Narrowband Internet of Things
NPBCH	Narrowband Physical Broadcast Channel
NPDCCH	Narrowband Physical Downlink Control Channel
NPDSCH	Narrowband Physical Downlink Shared Channel
NPSS	Narrowband Primary Synchronization Signal
NR	New Radio
NRS	Narrowband Reference Signal
NSSS	Narrowband Secondary Synchronization Signal
OFDM	Orthogonal Frequency-Division Multiplexing
OPEX	Operating Expenses
PA	Power Amplifier
PBCH	Physical Broadcast Channel
PCFICH	Physical Control Format Indicator Channel
PCID	Physical Cell Identity
PDCCH	Physical Downlink Control Channel
PDSCH	Physical Downlink Shared Channel
PHICH	Physical Hybrid ARQ Indicator Channel
PRB	Physical Resource Block
PSK	Phase-Shift Keying
PSS	Primary Synchronization Signal
QAM	Quadrature Amplitude Modulation
QPSK	Quadrature Phase-Shift Keying
QXDM	Qualcomm eXtensible Diagnostic Monitor
RBS	Radio Base Station
RF	Radio-Frequency
RSRP	Reference Signal Received Power
RU	Radio Unit
RX	Receiver

SFBC	Space-Frequency Block Coding
SFN	System Frame Number
SI	System Information
SIB	System Information Block
SIMO	Single-Input Multiple-Output
SISO	Single-Input Single-Output
SNR	Signal-to-Noise Ratio
SSS	Secondary Synchronization Signal
TDD	Time-Division Duplex
TX	Transmitter
UE	User Equipment
UL	Uplink
URLLC	Ultra-Reliable and Low-Latency Communication
VDC	Volts Direct Current
VoLTE	Voice over LTE

Chapter 1
Introduction

There is an increasing demand for wireless communication systems to not only provide communication between humans, but also between non-humans, i.e. things. This is commonly known as the Internet of Things (IoT). In the 3rd Generation Partnership Project (3GPP) release 13, the specification of a new low-cost Massive Machine Type Communication (mMTC) technology using a narrow bandwidth was frozen. This technology has the name Narrowband Internet of Things (NB-IoT). NB-IoT joined another already existing Cellular IoT (CIoT) technology standard called LTE-Machine Type Communication (LTE-M). Together, these two technologies are classified as Low-Power Wide Area Networks (LPWAN) technologies. It is estimated that by 2025, there will be 24.9 billion IoT connections globally, out of which, 5 billion will be CIoT. Out of these 5 billion CIoT connections, 52% are projected to be either NB-IoT or LTE-M [1].

Cellular networks were estimated to consume 0.97% of the total electricity grid supply in 2010, and by 2015, this had increased to 1.15% [2]. Energy consumption has been found to make up 20-40% of the Operating Expenses (OPEX) of networks for a Mobile Network Operator (MNO) [3]. This implies that there is a monetary incentive for operators to reduce the energy consumption of their networks, as this directly translates into reduced OPEX. In the simplest form, this lowers their electricity bill. Another great gain from reducing energy consumption is the increased sustainability for the telecommunication sector. In 2015, Information and Communications Technology (ICT) networks were estimated to be responsible for 0.34% of all carbon emissions globally [2], more than 3 times Sweden's yearly Carbon Dioxide (CO_2) emissions [4, p. 206]. Measurements done at Ericsson show that activating NB-IoT in a Long-Term Evolution (LTE) cell increases the power consumption of the Radio Base Station (RBS) by an unjustifiable amount. As NB-IoT aims to let operators support a rapidly growing demand for low-cost IoT connectivity, it is not enough that the devices are cheap, the increased expenses for the operators should also be low.

1.1 Objectives and Disposition

The purpose of this thesis is to investigate the reasons for the increased power consumption of an LTE RBS with NB-IoT operating in-band. The work includes describing, and comparing possible solutions aiming to lower this power consump-

tion.

The thesis begins in chapter 2 by giving a theoretical background to wireless communication technologies, and introducing existing power save features. In chapter 3 the energy consumption of mobile networks is investigated. Chapter 4 describes the methods used in the thesis and the investigation carried out. Further, this chapter also describes two new methods, out of which one was implemented and tested. Chapter 5 presents the results from the methods presented in chapter 4. A discussion of the results can be found in chapter 6 together with a conclusion and ideas for future work within this area.

Chapter 2
Theory

This chapter presents a theoretical background for concepts that were used for this thesis. Some will be described briefly, while others will be described more in detail.

2.1 Wireless Transmission

A wireless transmission system can be separated into senders and receivers. The sender, usually operated by an MNO, is the RBS, these are described more in detail in section 2.7. Receivers are devices, such as smart phones. These are commonly called User Equipment (UE). Downlink (DL) is when an RBS transmits to a UE, and Uplink (UL) is when a UE transmits to an RBS. The sending antenna is commonly referred to as the Transmitter (TX) and the receiving antenna as the Receiver (RX). These concepts are illustrated below in Figure 2.1.

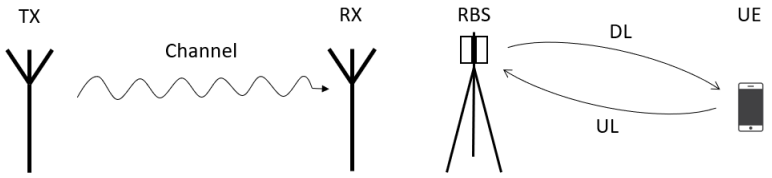

Figure 2.1: Illustration of transmitter and receiver (left) and communication between a radio base station and user equipment (right)

Information is sent using electromagnetic waves between the TX and RX. The space between the TX and RX, referred to as the channel, affects the transmitted signal. The effect on the transmitted signal differs depending on the frequency of the transmitted signal. This leads to the received signal looking different from the transmitted signal. The RX can attempt to estimate the alterations the channel made on the signal. One way of doing this is through sending reference signals. These are signals that are known to both the TX and RX, and by carrying out channel estimation on these signals, the RX will have an idea of the channel impulse

response. With the estimated channel properties, the RX can then process the received signal and attempt to recreate the transmitted signal.

2.2 Mobile Communication

Mobile communication, a technology which allows people around the world to communicate using electromagnetic waves, saw its first generation of a voice-only communication system in the 80s. This First Generation (1G) was an analog technology available nationally on a small scale. In the 90s, a new generation appeared, the Second Generation (2G). This was a digital technology which started out as voice-only but later evolved to support data transfer. By the end of the 90s, 2G had become the de facto global standard [5, p. 2].

Around this time, 3GPP was created to ensure that further developments of mobile communication technologies would be carried out as a global cooperation, rather than geographically separated as previously. Just at the turn of the millennium, Third Generation (3G) was finalized. This new generation offered not only voice, but also video services and data services. With later enhancements, 3G offered mobile-broadband capabilities.

With the introduction of a true mobile-broadband, users' expectations on high data rates and low latency grew. This in turn lead to the development of a new generation of mobile-communication technology, which could focus on high data rates and low latency as a core, rather than an enhancement as was the case with 3G. This new technology was Fourth Generation (4G) LTE, which was released in the late 00s. LTE has since seen multiple improvements, and is today the most successful mobile wireless broadband technology [5].

Even with the success of LTE, released in 2009, discussions about the next generation started just a few years later in 2012. These discussions on the Fifth Generation (5G) of mobile communication were centered on three use cases: Enhanced Mobile Broadband (eMBB), mMTC, and Ultra-Reliable and Low-Latency Communication (URLLC). In 2015, 3GPP started the development of a technology meant to deliver these use cases called New Radio (NR), with the first specification available in late 2017 [6]. One of the key requirements of this new technology is to offer enhanced capabilities without increasing the total energy consumption as compared to the networks operating today, which requires increased energy efficiency in the cellular networks [6, p. 18].

2.3 Duplexing

A communication system with both UL and DL is a duplex system. Two different types of duplex systems exist: full duplex and half duplex. Full duplex means that transmission is possible in both directions at the same time. Half duplex, in contrary, means that transmission is only possible in one direction at a time.

There are two duplex schemes, which aim to make transmissions in both directions possible for wireless communication systems. These are: Frequency-Division Duplex (FDD) and Time-Division Duplex (TDD). FDD separates DL and UL on

different frequency bands, and is illustrated to the left in Figure 2.2. This enables transmissions in both directions taking place simultaneously. FDD requires devices to be capable of receiving and transmitting on multiple frequency bands simultaneously. TDD uses one frequency band, but separates DL and UL in time slots. This means that in TDD it is not possible to transmit and receive simultaneously. TDD therefore does not require a device to be capable of receiving and transmitting simultaneously. TDD is illustrated to the right in Figure 2.2.

It is also possible for FDD to be half duplex. In this case, the device is not required to be able to receive and transmit simultaneously. The DL and UL is in this case separated in both frequency and time, which would result in a combination of the two illustrations in Figure 2.2.

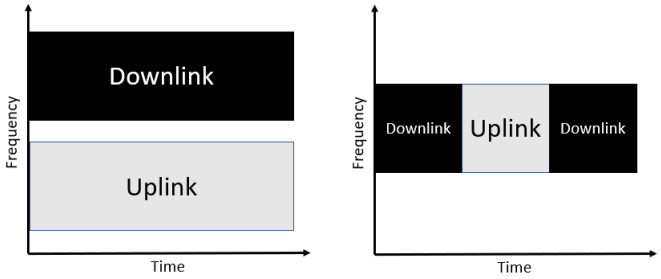

Figure 2.2: Frequency-division duplexing (left) and time-division duplexing (right)

LTE is able to use both FDD and TDD. In NB-IoT, the duplexing scheme supported was originally half duplex FDD, however, release 15 saw the addition of support for TDD in NB-IoT [7].

This thesis will only investigate NB-IoT using FDD.

2.4 Modulation

The bits to be transmitted from the sender to the receiver need to be mapped to a carrier frequency that can be transmitted over the air. This is accomplished through modulation. For example, transmitting at different frequencies depending on the bits to be transmitted, this is known as Frequency Modulation (fm). Another example is Phase-Shift Keying (PSK), where, as the name suggests, the phase is shifted to represent specific bit patterns. The simplest method of PSK would be to use two phase shifts, where each phase shift would be a symbol associated with one bit. In Quadrature Phase-Shift Keying (QPSK), there are four different phase shifts, which means that the system can encode two bits per symbol. This is commonly illustrated in a constellation diagram with a real, and an imaginary axis, with an example of a constellation diagram of QPSK shown below in Figure 2.3. In this context the real axis is called the in-phase (I) axis and the imaginary axis is called the quadrature (Q) axis. Each point in the diagram is a symbol which is associated with a specific bit pattern. For example, in the left

diagram in Figure 2.3, the top left point would be the symbol (-1, 1), and the bit pattern associated with this symbol could be 01.

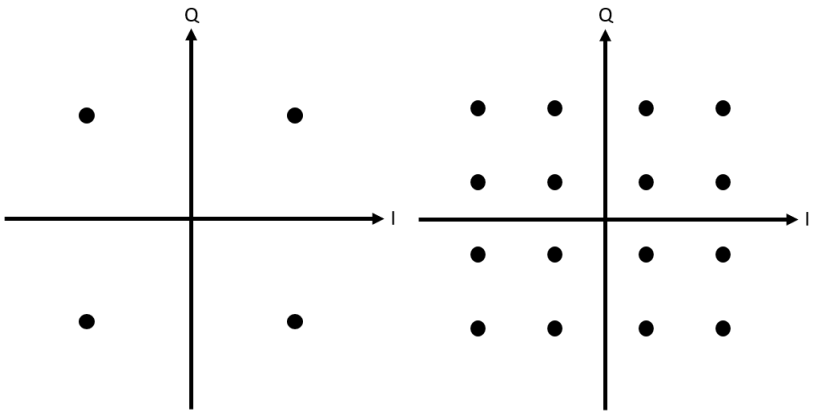

Figure 2.3: Constellation diagram of QPSK (left) and 16-QAM (right)

One method to add more symbols is by combining two carrier waves, commonly a cosine and a sine wave, and modulating the phase, and amplitude of these independently. This is called Quadrature Amplitude Modulation (QAM), which can be represented in a constellation diagram as shown in Figure 2.3. To accomplish 4 bits per symbol, 16-QAM is used. The name 16-QAM means that there are 16 symbols in the constellation diagram. In LTE, the maximum supported is 256-QAM which is intended for environments with a high Signal-to-Noise Ratio (SNR).

The reason why a high SNR is important for a higher order modulation scheme is that the symbols are closer to each other. A high SNR will lead to the received signal having a higher probability of being close to the transmitted signal. A low SNR would produce the opposite effect. The measurement of how far the received signal is from the transmitted signal is called the Error Vector Magnitude (EVM). This is therefore an important measurement when evaluating the performance of a wireless network.

2.5 Orthogonal Frequency-Division Multiplexing (OFDM)

Orthogonal Frequency-Division Multiplexing (OFDM) is a method for transmitting multiple QAM signals simultaneously in one signal. This is done through mapping each QAM signal to one frequency, a subcarrier. The subcarriers are spread over the channel bandwidth and are orthogonal to each other in the frequency domain. These multiple signals are then combined into one signal using an inverse Fourier transform. Figure 2.4 illustrates the frequency domain of an OFDM system. Four subcarriers can be seen in the figure, with the distance between each subcarrier being denoted as Δf. The orthogonality can be seen in that

at the maxima of each subcarrier, the other subcarriers have zero power. This is one of the ways that OFDM reduces Intersymbol Interference (ISI). The other way that OFDM reduces ISI is through the use of a cyclic prefix. After combining all of the subcarriers into an OFDM symbol, the end of the symbol is copied and added at the beginning [8].

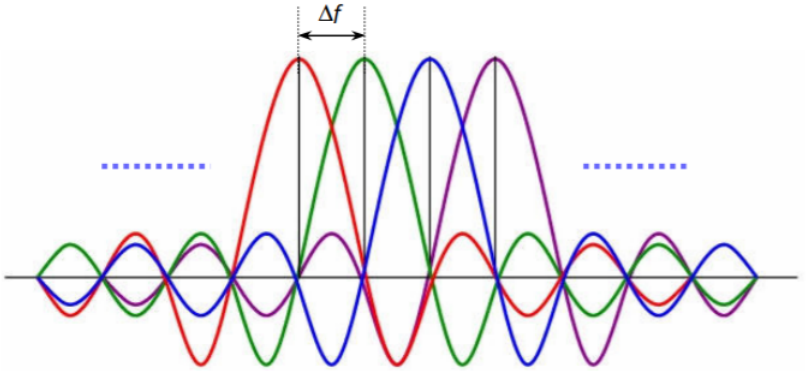

Figure 2.4: OFDM subcarriers, figure from [8]

The subcarrier spacing Δf is chosen such that $\Delta f = \frac{1}{T_{obs}}$ where $T_s = T_{obs} + T_{cp}$. T_s is the OFDM symbol time, and T_{cp} is the duration of the cyclic prefix. The T_{cp} should be chosen such that $T_{cp} \ll T_s$ and is larger than the channel impulse response [9].

At the RX, the cyclic prefix is removed, and the received OFDM symbol is separated into the component subcarriers using a Fourier transform. Through channel estimation, the received data is decoded and the symbols extracted from the QAM signals.

2.6 Multiple-Input Multiple-Output (MIMO)

Multiple-Input Multiple-Output (MIMO) uses multiple transmitting and receiving antennas to achieve a greater capacity in a wireless system. There is also Multiple-Input Single-Output (MISO), with a multiple transmitting antennas and a single receiving antenna, Single-Input Multiple-Output (SIMO), with a single transmitting antenna and multiple receiving antennas, and Single-Input Single-Output (SISO), with a single transmitting and receiving antenna.

The use of multiple antennas at the TX and RX gives array gain. This means that the received signal is stronger thanks to being able to combine the signals in the RX.

It is also possible to exploit the different paths the transmitted signals travel to the receiver to send multiple streams of data simultaneously. This is called spatial multiplexing. This is illustrated in the figure to the left in Figure 2.5.

Another feature of MIMO is diversity. This is achieved using orthogonal coding. This utilizes the different paths mentioned in spatial multiplexing, but instead

sends only a single data stream to the RX. The multiple paths ensure a higher probability that the data reaches the RX. This is illustrated to the right in Figure 2.5.

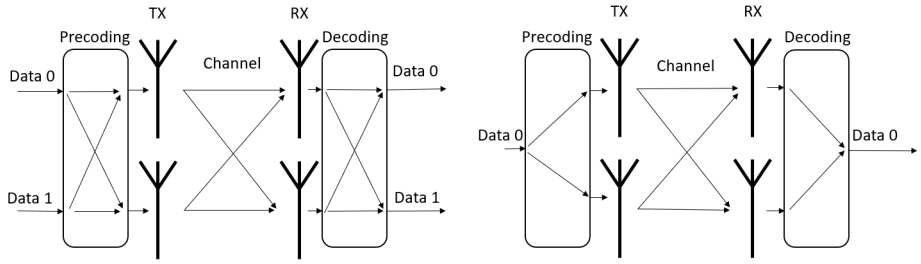

Figure 2.5: Simplified illustration of 2x2 MIMO with increased capacity (left), and diversity (right)

The antennas are placed such that they have an orthogonal polarization. By slanting each antenna element 45 degrees in either direction cross-polarization is achieved. In a MIMO system with 4 antennas, the antenna would be made up of two crosses of two antenna elements each, spatially separated to achieve spatial multiplexing. Two cross-polarized antenna elements are illustrated in Figure 2.6.

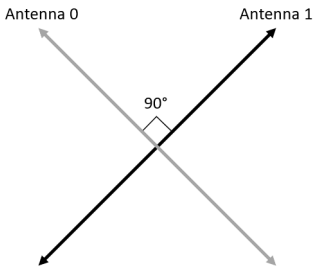

Figure 2.6: Simplified illustration of 2 cross-polarized antenna elements

2.7 Radio Base Station (RBS)

An RBS is made up of three components: the Digital Unit (DU), the Radio Unit (RU) and the antenna. The DU, also called the baseband, codes downlink transmissions and decodes received uplink signals. The output from the DU is transmitted to the RU which converts the signal to the correct frequency and amplifies it. This radio signal is then sent to the antenna which transmits it to the UE. For receiving uplink, the same process is done in reverse.

One RBS typically makes up one network cell. A cell is usually made up of three sectors covering 120° each [10, p. 384]. To accomplish this, each RBS will

have three antennas with one RU each. As seen in Figure 2.7, this setup gives the cell a hexagon shape, which is chosen as this allows the highest density of cells without overlap.

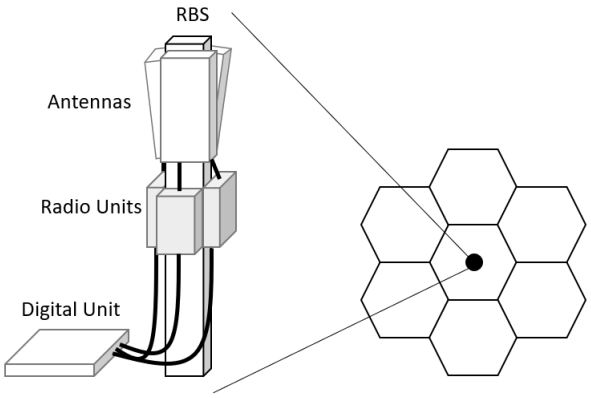

Figure 2.7: RBS illustrated as one hexagonal cell in a network

There exists many circumstances in which a cell would see huge differences in traffic in an easily predictable way. For example, a cell covering a venue would see an increase in traffic during events, and a cell covering a summer resort would see its traffic increase during the summer. A way to increase the capacity in these places without increasing the density of RBSs is by placing multiple cells on the same RBS, separated in frequency. One coverage cell, usually on a lower frequency band with better propagation characteristics, and one capacity cell, or more if necessary, that can be turned on when the traffic in the coverage cell exceeds a certain threshold or a scheduled event is taking place.

2.8 Long-Term Evolution (LTE)

LTE uses OFDM as the basic transmission scheme for both DL and UL [5, p. 75]. Although LTE supports both FDD and TDD, this thesis, and therefore this section, will focus on FDD DL.

2.8.1 Time-Frequency Structure

The subcarrier spacing used in LTE is 15 kHz, which was chosen as it offered a good balance between the length of cyclic prefix, to handle ISI, and frequency errors between the TX and RX, such as Doppler shift [5, p. 75]. Looking at the LTE resource grid in terms of subcarriers is usually referred to as the frequency domain. The time domain is, as the name suggests, the resource grid over time.

Figure 2.8 shows how the time domain and frequency domain relate to each other to form the LTE frame structure. LTE transmissions are separated into frames of 10 ms. Each frame is made up of 10 subframes of 1 ms each. One

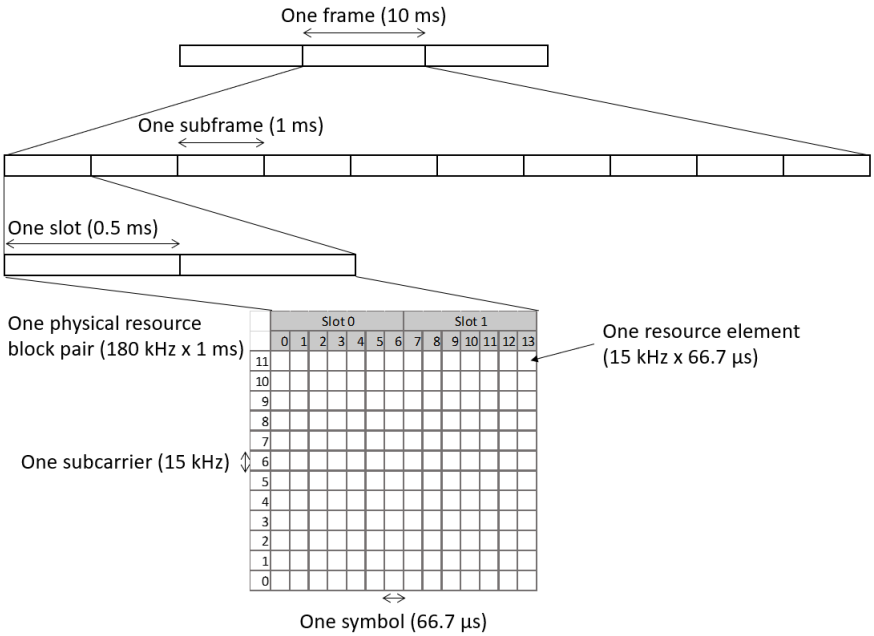

Figure 2.8: LTE time domain structure and time-frequency frame structure

subframe contains two slots of 0.5 ms each. One slot is 7 symbols with the approximate symbol time 66.7 μs. This symbol time includes the cyclic prefix mentioned previously. One symbol time over one subcarrier is one resource element. Subcarriers are grouped together in groups of 12. The smallest schedulable unit is one Physical Resource Block (PRB) pair, which is 12 subcarriers over two slots.

2.8.2 Downlink Signals and Physical Channels

This section will list and briefly describe the signals and physical channels which are relevant to this thesis. Figure 2.9 contains a visual representation of where in the LTE resource grid the following signals and physical channels are found.

Physical Broadcast Channel (PBCH)

The PBCH is used to transmit the System Information (SI) which the UE uses to access the network.

Physical Downlink Control Channel (PDCCH)

The purpose of the PDCCH is to transmit Downlink Control Information (DCI) to the UE. The DCI contains scheduling information and scheduling grants for uplink transmission. The length of the PDCCH depends on the amount of control information to be transmitted.

Physical Control Format Indicator Channel (PCFICH)

The PCFICH informs the UE how to decode the PDCCH.

Physical Hybrid ARQ Indicator Channel (PHICH)

The PHICH transmits the hybrid-Automatic Repeat reQuest (ARQ) to the UE which informs the UE if the transmission of a transport block was successful or not. If the transmission was unsuccessful, a retransmission is scheduled.

Physical Downlink Shared Channel (PDSCH)

The main purpose of the PDSCH is to transmit data intended for a single user, but it is also used for transmitting paging information.

Primary Synchronization Signal (PSS)

The PSS is used for the UE to discover the cell, it also provides the UE with timing information. There are three different PSSs available, given by the Physical Cell Identity (PCID).

Secondary Synchronization Signal (SSS)

The SSS can be decoded by the UE after finding the PSS. There are 168 different SSSs. Combining the identity of the SSS and the PSS tells the UE which cell-identity group the cell has. The UE will also be able to deduce the frame timing from this and make it possible to decode the PBCH.

Cell Specific Reference Signal (CRS)

The CRS is a signal known to both the TX and RX which is used to carry out channel estimation. It will also inform the UE how good the reception is which the UE can use to compare different network cells. For both 2TX and 4TX LTE modes, meaning the RBS uses either 2 or 4 transmitting antenna ports, there is one specific CRS transmitted on each antenna. This means that the RX can know which CRS originates from which transmitting antenna port. Clever placement and puncturing ensures that two antennas' CRSs do not interfere with each other.

2.8.3 LTE Resource Grid

This section provides an example of what an LTE FDD resource grid looks like. Figure 2.9 shows what the smallest possible bandwidth of an LTE network, 1.4 MHz looks like. It is made up of 6 PRBs. The largest possible bandwidth is 20 MHz which would be 100 PRBs [5, p. 490].

The resource grid in Figure 2.9 shows the contents of a frame in an idle LTE cell. There is an error in this figure, where the CRS are supposed to be red, but are actually black, use Figure 2.10 to distinguish which resource elements contain CRSs. As the cell is idle, there are no scheduled transmissions to any UEs. There are multiple symbols that are occupied anyway. The signals and physical channels

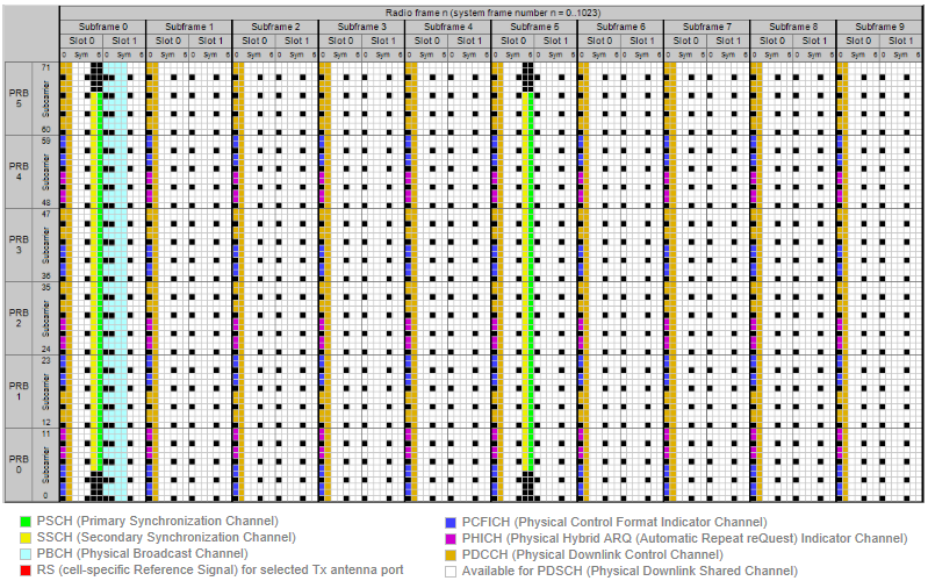

Figure 2.9: LTE FDD Frame Structure, figure from [11]

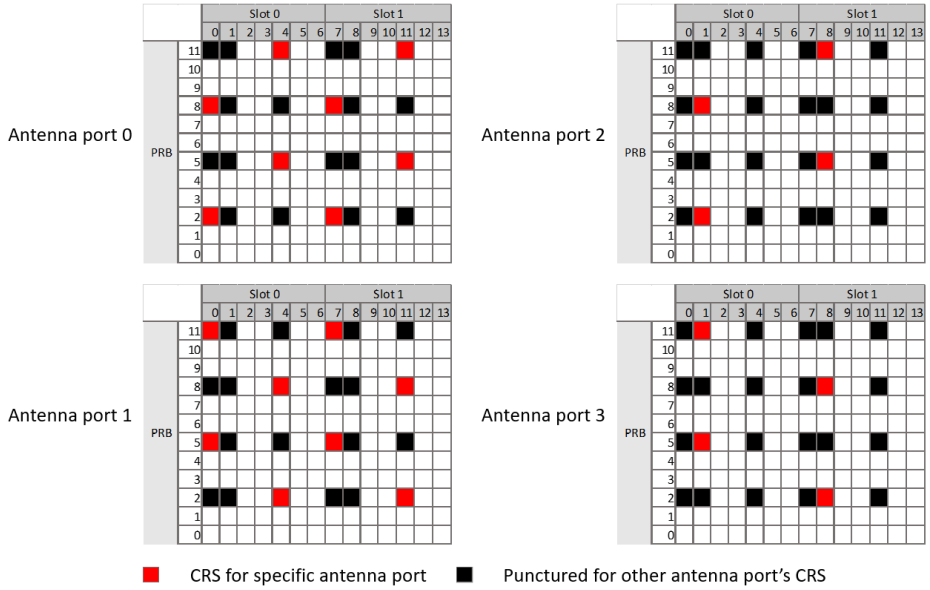

Figure 2.10: CRS placement and puncturing for each antenna port in 4TX LTE

found in these symbols can be called "always on". For example, in the figure, it is clear that there are 4 CRSs per subframe, this means that this is a 2TX cell, in one subframe, each antenna transmits their corresponding CRS four times. A 4TX

cell would contain 6 CRSs per subframe. Figure 2.10 illustrates the placement of CRS in an LTE cell with four antenna ports. Here, antenna ports 0 and 1 will transmit their CRS four times, while antenna ports 2 and 3 transmit their CRS twice per subframe.

With only two antenna ports configured, the CRS and puncturing seen in antenna ports 2 and 3 in Figure 2.10 would be available to other physical channels. As seen, with this placement and puncturing, it is ensured that two antenna ports never transmit a CRS at the same time and frequency.

2.9 Internet of Things (IoT)

IoT is described by Liberg et al. [12, p. 2] as "the latest rising star in the information and communications technology (ICT) industry and embodies the vision of connecting virtually anything with everything". As previously stated, it is estimated that there will be 24.9 billion IoT connections globally by 2025, a sharp increase from the current 10.8 billion existing connections [1]. Liberg et al. [12, p. 2] further writes that connectivity over cellular networks is a key enabler for the growth of the number of connected devices. IoT over cellular networks can be called CIoT. One CIoT technology is the LPWAN technology NB-IoT which this thesis was focused on.

2.10 Narrowband Internet of Things (NB-IoT)

NB-IoT was designed to meet high requirements on coverage, capacity, and battery lifetime [12]. Another requirement was that it should be possible to operate NB-IoT in old Global System for Mobile Communications (GSM) frequency bands of 200 kHz. The solution to this was a technology that built heavily upon the already existing LTE technology. In fact, NB-IoT is a part of the 3GPP LTE specification [12, p. 220]. NB-IoT utilizes the same OFDM technology as LTE, but is confined to a single PRB, which with its 180 kHz bandwidth makes it possible to fit in an old GSM frequency band. Originally only designed for FDD, recently TDD was added. However, this report will only consider NB-IoT FDD.

This section seeks to describe the aspects of NB-IoT that apply to the work of this thesis.

2.10.1 Downlink Signals and Physical Channels

There are six different signals and physical channels in NB-IoT DL. Five of these are time-multiplexed by being assigned to specific subframes in every frame. This is illustrated in Figure 2.11. The sixth signal, the Narrowband Reference Signal (NRS), is transmitted in almost every subframe, with the exact subframe depending on the operation mode. At a minimum, NRS is present in all subframes that can carry Narrowband Physical Downlink Control Channel (NPDCCH) and Narrowband Physical Downlink Shared Channel (NPDSCH), even if neither are scheduled to contain any data. In the case of in-band operation mode, NRS is

also present in subframe 0 carrying the Narrowband Physical Broadcast Channel (NPBCH).

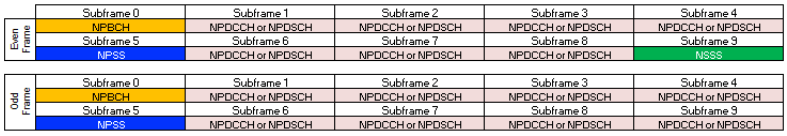

Figure 2.11: Channel allocations within a radio frame, figure from [16] corrected

NPBCH

The purpose of the NPBCH is to transmit the Master Information Block - Narrowband (MIB-NB) to the UE, and is transmitted in subframe 0 of every frame. The MIB-NB contains essential information about the NB-IoT cell which the UE needs to use the network.

NPDCCH

The NPDCCH carries DCI to the UE. This contains information on UL grants, DL scheduling, and paging indication or SI updates. In order for the UE to detect any DCI intended for it, the UE must know where to search for the NPDCCH. The possible locations for the NPDCCH are known as the NPDCCH search spaces.

NPDSCH

The NPDSCH is used to transmit data to the UE from higher layers. It is also used to broadcast SI to all UEs in the cell.

Narrowband Primary Synchronization Signal (NPSS)

The NPSS is used by the UE to synchronize with the NB-IoT cell in time and frequency. Unlike in LTE where there are three different PSSs, NB-IoT only uses one NPSS. This means that all NB-IoT cells use the same NPSS, this lowers the device complexity for NPSS detection.

Narrowband Secondary Synchronization Signal (NSSS)

The NSSS lets the UE obtain further cell information after the NPSS has been detected. After successfully matching the received NSSS the UE will know which of the 504 unique PCIDs the cell has. Further, the UE will also know the three least significant bits of the System Frame Number (SFN).

NRS

The NRS is used for the UE to carry out channel estimation and to measure the signal strength. As mentioned above, it is present in almost all subframes. Its position in the subcarriers is shifted depending on the cell identity to ensure that two adjacent cells' NRSs are orthogonal, and in case of operating in-band, matches the subcarrier position of the enclosing LTE cell's CRSs.

2.10.2 Carrier Types

NB-IoT allows for two types of carriers. The anchor carrier and the non-anchor carrier. An anchor carrier contains all signals and physical channels mentioned above. A non-anchor carrier can be used to increase the capacity of the NB-IoT cell by introducing a new carrier which only carries NPDCCH and NPDSCH, increasing the downlink capacity without the overhead of transmitting multiple NPSS, NSSS, NPBCH. Multiple non-anchor carriers can be added to an NB-IoT cell with an already existing anchor carrier. These non-anchor carriers can be dynamically opened and closed to allow the cell to adapt to the level of NB-IoT traffic on the network.

If multi-carrier operation is possible, the UE camps on the anchor carrier and monitors paging messages until it is required to switch to connected mode. When this happens, the anchor carrier assigns the UE to a non-anchor carrier and sends the information necessary about the non-anchor carrier. The UE can then connect to the assigned non-anchor carrier and carry out all DL and UL signaling. Upon completion, the UE can camp on the anchor carrier again and switch back to idle mode.

2.10.3 Operation Modes

NB-IoT can operate in three modes: in-band, guardband, and stand-alone. With the modes in-band and guardband, NB-IoT piggybacks on an already existing LTE cell, while in stand-alone, as the name suggests, NB-IoT operates by itself, for example in a refarmed GSM band. These different modes are illustrated in Figure 2.12.

For this thesis, the focus is on NB-IoT operating in the in-band mode.

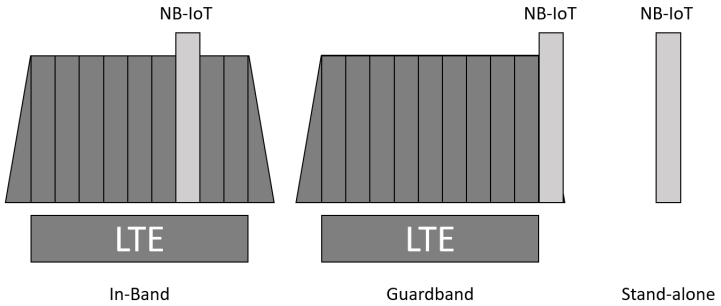

Figure 2.12: NB-IoT operation modes

In-Band

When NB-IoT operates in the in-band operation mode, and therefore shares its resource grid with its enclosing LTE carrier, NB-IoT must be able to handle when the LTE uses an equal amount of antenna ports, or more. In-band NB-IoT handles this by puncturing its resource grid with empty symbols for the LTE PDCCH and LTE CRS.

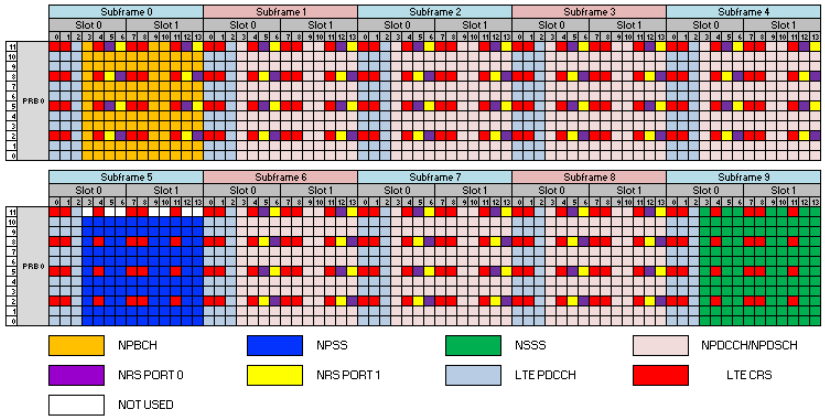

Figure 2.13: Even frame structure for in-band NB-IoT FDD, figure from [16]

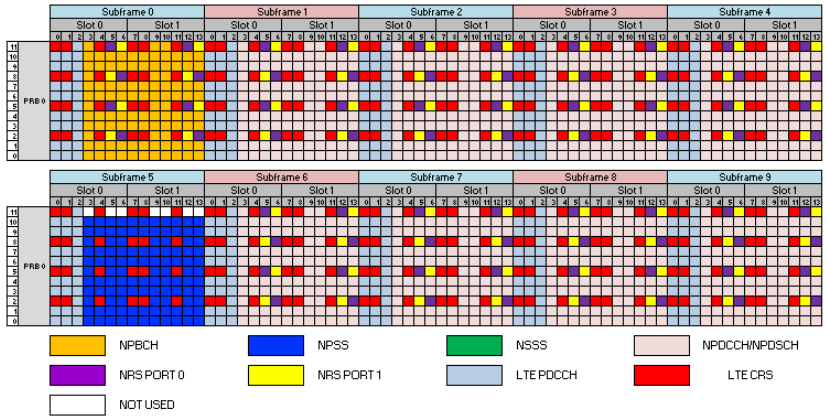

Figure 2.14: Odd frame structure for in-band NB-IoT FDD, figure from [16]

Pictured in Figures 2.13 and 2.14 is what the resource grid for an in-band NB-IoT anchor carrier in an LTE cell with two or more antenna ports looks like. As seen in the figures, NB-IoT adds two reference signals, NRS 0 and NRS 1 for each antenna port respectively. These are added in the resource grid in a fashion that does not introduce any interference with the LTE cell's CRS. These CRS

symbol positions are punctured in the NB-IoT resource grid. If compared to the CRS placements in Figure 2.10, it can be seen that the NB-IoT in-band resource grid is punctured to be able to be used in-band in a 4TX LTE cell.

Guardband

As suggested by the name of this operation mode, NB-IoT guardband mode means that the NB-IoT carrier is placed in the guardband of an LTE cell's bandwidth. The occupied bandwidth of an LTE carrier is only about 90% of the channel bandwidth, there is therefore about 5% of the channel bandwidth available on each side for NB-IoT in guardband mode [12].

Since there is no need to puncture for LTE signals, the resource grid looks different as compared to the one presented above for in-band. The resource grid for guardband can be seen in Figures 2.15 and 2.16. The lack of PDCCH and CRS means that there will be more space in the resource grid for NPDCCH and NPDSCH.

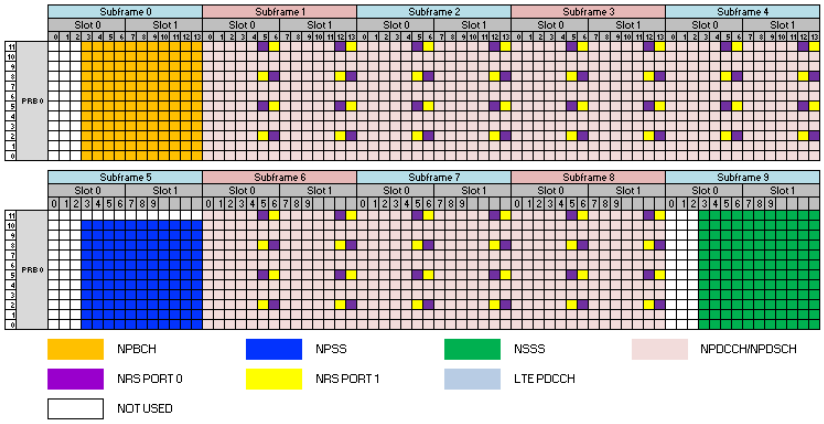

Figure 2.15: Even frame structure for guardband and stand-alone NB-IoT FDD, figure from [16]

Stand-Alone

In NB-IoT stand-alone mode, there is no LTE carrier to take into account at all. This results in the same resource grid being used as for the guardband mode. Stand-alone and guardband therefore share the resource grid presented in Figures 2.15 and 2.16.

2.10.4 Coverage Extension

NB-IoT was designed to handle a Maximum Coupling Loss (MCL) of 164 dB. The MCL is the maximum loss that the system can handle and still be operational. This is 20 dB more than the cell edge of a GSM cell. One of the ways in which this is accomplished is through repetitions. When the MCL increases above a certain

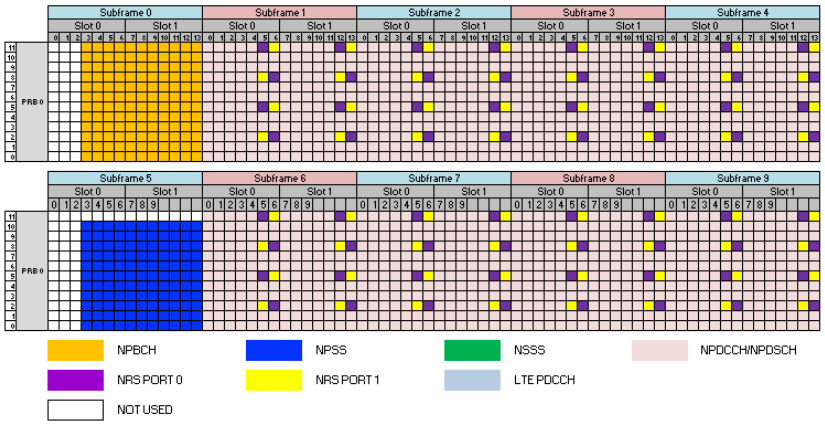

Figure 2.16: Odd frame structure for guardband and stand-alone NB-IoT FDD, figure from [16]

threshold, the number of repetitions will increase. This makes it possible to detect transmissions with a very low SNR. Another method used to extend the coverage is PRB boosting. This is always used in anchor carriers, but is not required in non-anchor carriers [12, p. 301]. For example, in a 10 MHz LTE cell with NB-IoT operating in-band, the PRB with the NB-IoT anchor carrier will be boosted by 6 dB. This can be accomplished by, for instance, using 4 PRBs available power to transmit 1 PRB. This will lead to there being 4 times more power available for the NB-IoT PRB, which is a 6 dB increase.

2.10.5 Antenna Mapping

NB-IoT is able to operate with either one or two logical antenna ports. A simple approach is that one logical antenna port is mapped to one physical antenna. In NB-IoT however, it is up to the implementation how the logical antenna ports are mapped to the physical antennas [12, p. 232]. When two logical antenna ports are used, NB-IoT uses Space-Frequency Block Coding (SFBC) to gain transmit diversity. How this works is shown below in Figure 2.17, where s_i is the i:th symbol to be transmitted, and s_i^* denotes the complex conjugate of i:th symbol s.

As seen in Figure 2.17 above, each symbol s is transmitted twice, separated both in space and frequency, hence the name of the coding scheme. Transmitting like this is a type of Alamouti coding, and as NB-IoT devices are expected to have a single receiving antenna [12, p. 232], this scheme extracts a full transmit diversity order of 2 [21]. This mapping is also shown below in equation 2.1 [12, p. 232].

$$\begin{bmatrix} x_{2i}^0 \\ x_{2i}^1 \\ x_{2i+1}^0 \\ x_{2i+1}^1 \end{bmatrix} = \frac{1}{\sqrt{2}} \begin{bmatrix} 1 & 0 & j & 0 \\ 0 & -1 & 0 & j \\ 0 & 1 & 0 & j \\ 1 & 0 & -j & 0 \end{bmatrix} \begin{bmatrix} \mathrm{Re}(s_{2i}) \\ \mathrm{Re}(s_{2i+1}) \\ \mathrm{Im}(s_{2i}) \\ \mathrm{Im}(s_{2i+1}) \end{bmatrix} = \frac{1}{\sqrt{2}} \begin{bmatrix} s_{2i} \\ -s_{2i+1}^* \\ s_{2i+1} \\ s_{2i}^* \end{bmatrix} \tag{2.1}$$

where two symbols s_{2i} and s_{2i+1} are mapped at a time to precoded symbols x_{2i}^p

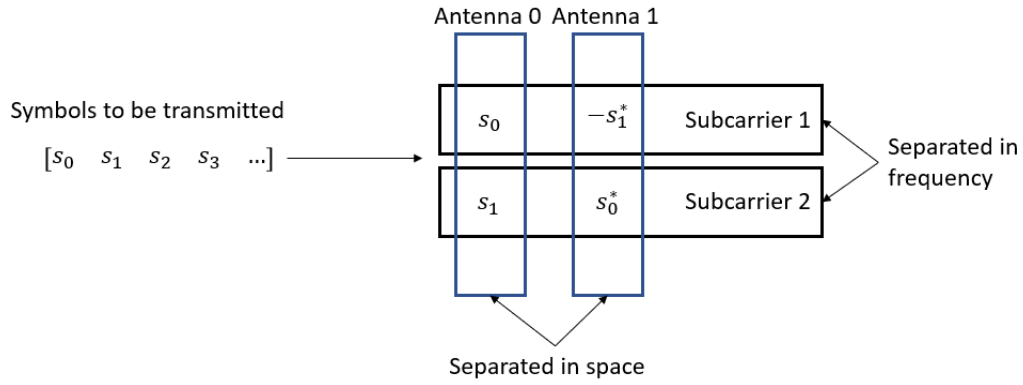

Figure 2.17: Space-Frequency Block Coding in NB-IoT

and x_{2i+1}^p where p is the antenna port. These symbols are transmitted over the channel as seen in Figure 2.18, where symbols s_0 and s_1 are used as an example.

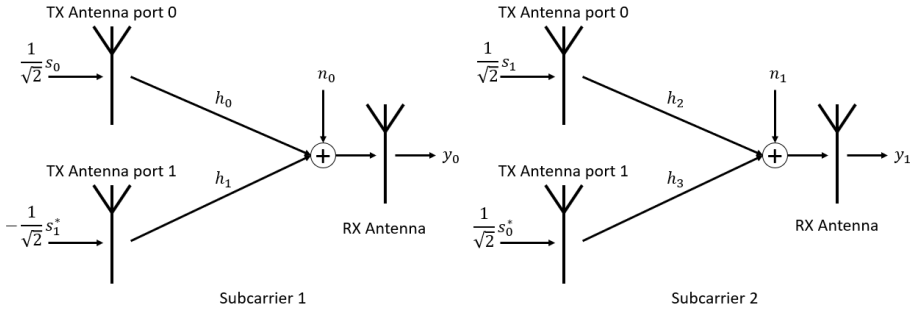

Figure 2.18: Transmission of SFBC coded symbols in 2TX NB-IoT

In Figure 2.18, h_0 and h_1 denote the channels from antenna ports 0 and 1 and the receiving antenna respectively on subcarrier 1, h_2 and h_3 denote the channels between antenna ports 0 and 1 respectively and the receiver on subcarrier 2. n_0 and n_1 denotes the noise at the receiver. The received signals y_0 and y_1 can be written as follows in equations 2.2 and 2.3 respectively.

$$y_0 = \frac{1}{\sqrt{2}}h_0 s_0 - \frac{1}{\sqrt{2}}h_1 s_1^* + n_0 \tag{2.2}$$

$$y_1 = \frac{1}{\sqrt{2}}h_2 s_1 + \frac{1}{\sqrt{2}}h_3 s_0^* + n_1 \tag{2.3}$$

These two received signals are combined as seen below in equation 2.4.

$$\mathbf{y} = \begin{bmatrix} y_0 \\ y_1^* \end{bmatrix} = \frac{1}{\sqrt{2}} \begin{bmatrix} h_0 & -h_1 \\ h_3^* & h_2^* \end{bmatrix} \begin{bmatrix} s_0 \\ s_1^* \end{bmatrix} + \begin{bmatrix} n_0 \\ n_1^* \end{bmatrix} = \frac{1}{\sqrt{2}}\mathbf{H}\mathbf{s} + \mathbf{n} \tag{2.4}$$

By doing channel estimation, the receiver can then approximate the channel $\mathbf{H}$ and use this estimation to approximate the transmitted symbols. This approximation $\mathbf{z}$ is obtained by multiplying $\mathbf{y}$ with the Hermitian transpose of $\mathbf{H}$ denoted as $\mathbf{H}^{\mathrm{H}}$.

$$\mathbf{z} = \frac{\mathbf{H}^{\mathrm{H}}\mathbf{y}}{||\mathbf{H}||^2} \tag{2.5}$$

How close the approximated symbol vector $\mathbf{z}$ is to the transmitted symbol vector $\mathbf{s}$ depends on the accuracy of the channel estimation and the SNR.

2.11 Power-Saving Features

This section seeks to describe some of the multiple power-saving features available in the Ericsson portfolio for 4G and 5G networks. More information on Ericsson's work on lowering the power consumption in mobile networks can be found in [17]. This thesis will investigate how some of these can be used or expanded in an NB-IoT network operating in-band in an LTE cell.

Micro Sleep TX (MSTX)

Micro Sleep TX (MSTX) is a feature that turns off the RU's Power Amplifier (PA) in DL during symbol times when all resource elements on all subcarriers are empty from data or signaling. Since nothing is to be transmitted during these symbol times, it is not necessary for the PA to be powered on. This enables power savings during low traffic [17].

Low Energy Scheduler Solution (LESS)

Low Energy Scheduler Solution (LESS) is a feature that attempts to give MSTX more empty symbol times. By buffering non-critical data, and waiting until a certain threshold or time-sensitive data before scheduling, the data can be spread out over all subcarriers rather than in time. This will give MSTX more opportunities to lower the power consumption. While the latency of time-insensitive data increases slightly, the latency of time-sensitive data, such as Voice over LTE (VoLTE), is not affected, maintaining quality of service [17].

MIMO Sleep Mode (MSM)

MIMO is used to increase the capacity by transmitting using multiple antennas. When there is low traffic, MIMO Sleep Mode (MSM) can lower the power consumption by switching to SIMO by turning off antennas. This will also decrease the capacity of the cell. When the traffic increases, the cell can increase the capacity by going back to MIMO again.

Cell Sleep Mode (CSM)

Cell Sleep Mode (CSM) is a feature that is available in networks where there are both coverage cells and capacity cells. CSM deactivates capacity cells when there is low traffic in the network and brings it back up again when traffic increases.

Massive MIMO Sleep Mode (mMSM)

Massive MIMO Sleep Mode (mMSM) works similarly to MSM, but for the massive MIMO case in 5G. This feature will not be considered in this thesis as the focus will be on NB-IoT operating in-band in an LTE cell.

Chapter 3
Network Power Consumption

This chapter presents a background of the power consumption of LTE networks.

3.1 RBS Power Consumption

In order to increase the energy efficiency of the RBS it is important to know how the power consumption behaves during operation. Figure 3.1 shows the power usage of an RBS over the Radio-Frequency (RF) output power. The RF output power is proportional to the load in the network. Maximum output power will be reached when the load in the network is 100%.

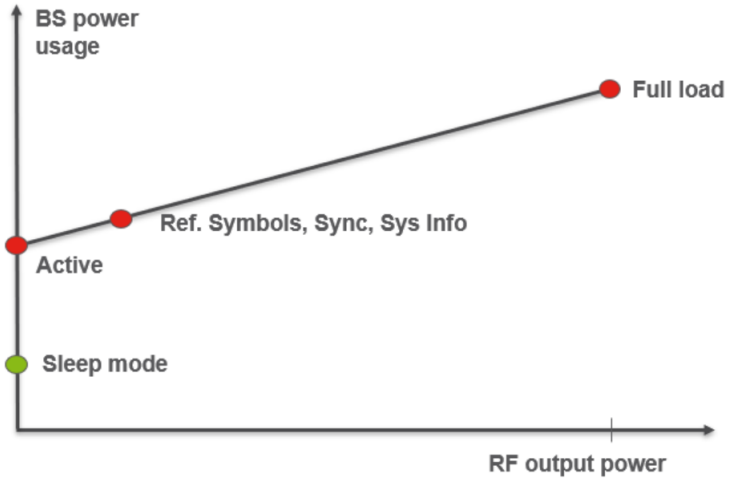

Figure 3.1: Power consumption of a radio base station, from [13]

As seen in Figure 3.1, with zero load, even activating the cell increases the power usage. However, at the minimum, the "always on" signals must be transmitted for the cell to be discoverable by UEs. This would place the power usage at the second red marker from the left in Figure 3.1. The power usage will then increase as the load increases. During sleep mode, the cell is not discoverable by UEs. It is beneficial for energy efficiency purposes to have the power usage scale

better with the load, and to strive to move the power usage at zero load closer to the power usage at sleep mode.

3.1.1 RBS Power Consumption Breakdown

Alsharif et al. [14] have shown that the base station makes up 57% of the power consumption of a cellular network. Out of which, the biggest part of the power is consumed by the PA. This is shown in Figure 3.2.

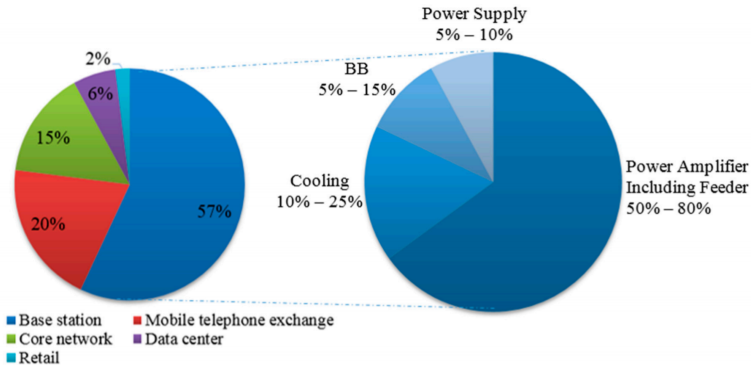

Figure 3.2: Power consumption of a wireless cellular network (left), and power consumption distribution in a base station (right), from [14]

There is also a positive feedback in this, where if the power consumption of the other components decrease, the amount of cooling necessary will decrease.

3.2 Network Traffic Pattern

In previous work done by Ericsson, it was found that only a few cells actually see high load in a network [13]. What this means is that most cells rarely need to transmit at full output power. Further research showed that this same pattern would be seen in the different environments usually used to generalize the areas cellular networks operate in: urban, suburban, and rural, which in turn are shown in Figure 3.3. This figure shows the sites in different environments sorted by their traffic. What is shown is that only a few sites see high traffic in each environment. This shows the necessity of finding a way to lower the power consumed when networks are idle, or at low load.

It was also shown that data is transmitted sporadically and not continuously when there is less than 100% load in the cell. This means that small pauses can be seen between each transmission, which is clarified in Figure 3.4.

In an LTE cell, this would mean that not every subframe in Figure 2.9 has data, and therefore, some symbol times are entirely empty of transmitted signals. The symbol times empty are the ones without the "always on" signals previously mentioned.

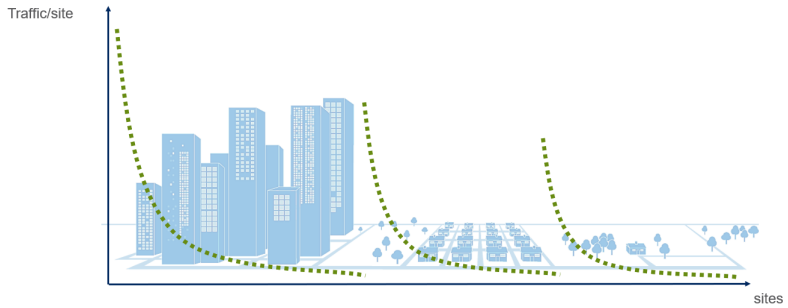

Figure 3.3: Visualization of traffic in areas: urban (left), suburban (middle), rural (right), from [13]

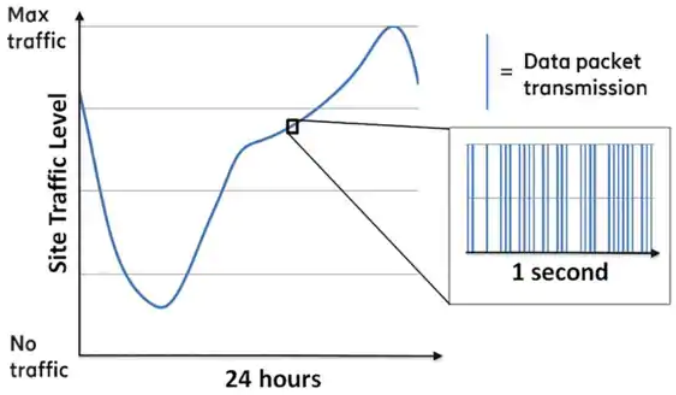

Figure 3.4: Visualization of traffic over 24 hours, from [13]

3.2.1 Existing power-saving features

These facts are exploited by MSTX, which turns off the PA in the radio unit when a symbol time over the whole bandwidth is empty, and no signal needs to be transmitted. LESS seeks to increase the number of times this happens by decreasing the density seen in Figure 3.4 while maintaining the same throughput.

This shows that there is a possibility to decrease the power consumption in a cell running NB-IoT if it is possible to increase the frequency of empty symbol times so that MSTX is able to turn off the PA more often.

Chapter 4
Method

This chapter details the investigation that was carried out into finding ways of decreasing the power consumption of an LTE cell running NB-IoT in-band. Two methods were found, antenna port muting, and Downlink Subframe Deactivation (DSD), both of which will be presented in this chapter.

4.1 Environment Setup

To be able to study the power consumption of an RBS, an environment was set up in the lab at Ericsson in Lund. This environment consisted of an Ericsson Baseband 5216 connected to an Ericsson Radio 1. The output signals from the radio's 4 antenna ports are then connected through an attenuator and a combiner to an NB-IoT UE, the MDM9206 IoT modem, made by Qualcomm. Connecting a UE to the environment enables verification of the cell's functionality. A Keysight 34401A multi-meter is used to measure the power consumption of the radio unit. The baseband unit can be monitored remotely from a laptop using the software MoShell. The laptop was also connected to the multi-meter for power measurements. The UE was connected to a desktop in the lab and Qualcomm eXtensible Diagnostic Monitor (QXDM) was used to monitor the performance of the connection. A simplified view of the setup can be found in Figure 4.1.

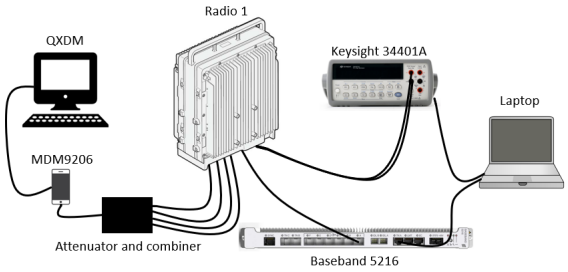

Figure 4.1: Simplified view of lab setup

Radio 1 is a dual band 4TX 20 W RU. This means that the RU has 4 antenna ports, operates on band A and band B, the real bands masked to ensure confidentiality, and has 20 W maximum RF output power per antenna port and band. In

this thesis, only band A was configured with a bandwidth of 10 MHz. Another thing worth noting is that the power-saving feature MSTX was activated in all measurements.

4.1.1 Power Measurement

The power consumption is measured using the Keysight 34401A multi-meter. The radio is supplied with -48 Volts Direct Current (VDC), which is adjusted to account for the voltage drop. To measure the current, the voltage drop is measured over a 4-poled shunt resistor. The current is then calculated by using Ohm's law, where I is the current in Ampere (A), V is the voltage in Volt, and R is the resistance in Ohm (Ω). Ohm's law is seen in equation 4.1

$$I = \frac{V}{R} \tag{4.1}$$

To get the average power consumption, the current and voltage is measured and calculated multiple times over a set period of time, e.g. 5 seconds. The average is then calculated and the average power consumed in Watt (W) is given by equation 4.2

$$P = V \cdot I \tag{4.2}$$

Energy is power over time and is often given as kilowatt-hour (kWh) which is the power consumed in one hour. For example, a 1000 W device running for an hour consumes 1 kWh.

4.1.2 Baseband Software Environment

In order to be able to investigate and implement new features in the baseband unit, it was necessary to gain access to the baseband software source code. The source code, written in C, was accessed through a virtual environment and was altered and built remotely. After building the new software, it was possible to install it on the local baseband unit as a patch.

Before making any alterations in the code, it was necessary to study it and learn how the hardware worked. Through the investigation carried out, which is presented in section 4.3, it was realized that most alterations would be done on layer 1, the physical layer, in the baseband software. This required an understanding of how the software interacts with the hardware, and a lot of time was spent on learning about how the digital signal processors work and the different types of memories used.

As changes were made on layer 1, it was necessary to find a way to interact with the software during run-time. In order to make something that can be interacted with through MoShell, it would have been necessary to carry out larger alterations in more parts of the source code. Rather than do this, it is possible to create a global variable which is mapped to a specific address in the common memory shared by all digital signal processors. After compilation, a map file is created from where it is possible to find this memory address. During run-time, it is possible to read and write to this memory address. This was used to verify that

the loading of the new, altered software was successful through reading a variable set to display a unique value in the software created for this thesis. It was also used to toggle the power saving features implemented in this thesis on or off by writing a specific value to a global variable.

It was decided that the new software was functional when a UE was able to attach to the cell, and it was possible to successfully ping another computer connected to the lab network. This was accomplished by using the UE, MDM9206 as a modem for the lab desktop computer. The quality of the connection was measured by using Reference Signal Received Power (RSRP), which is reported by QXDM. The RSRP is a measurement of the power of the reference signals over the bandwidth.

4.2 Energy Model

In order to calculate the effects of a power saving feature, it is necessary to have some kind of model for it. In this thesis, a simple model will be used to gain some insight into the monetary and environmental impacts of the power saving features investigated.

This thesis will only investigate power consumed by the RU. It will be assumed that each base station consists of three RUs. To get an idea of the power consumption in a network, it will be assumed that the whole network uses identical RUs, and that all RUs see the same effect from the power saving features. Further, the cost per kWh and the environmental impact will be based on the average in the USA. For this thesis, an example network consisting of 100 000 RBSs will be used.

4.2.1 Cost per kWh

The cost per kWh in the USA was found to be 10.29 cents in 2020 [18]. This equals \$0.1029 per kWh.

4.2.2 Carbon Dioxide (CO2) per kWh

The amount of CO_2 emitted by the electric power industry was found to be about 0.99 pounds per kWh in 2018 [19]. This equals 0.449 kg of CO_2 per kWh. In order to provide a frame of reference for the carbon emission, the average carbon footprint of a US household will be used. This carbon footprint has been estimated as 48 tons of CO_2-equivalents per year [20].

4.3 Investigation

In this section the investigations made into the power consumption and function of an LTE cell running NB-IoT in-band are presented.

4.3.1 Micro Sleep TX

A second lab environment was used to capture images of what the output signal from the RU looks like with MSTX activated. This environment will not be

described in detail. An oscilloscope was used to monitor both the output signal from the RU, as well as the signal MSTX uses to turn the PA on and off. Images of this running in a 4TX LTE cell is provided in Figures 4.2 and 4.3.

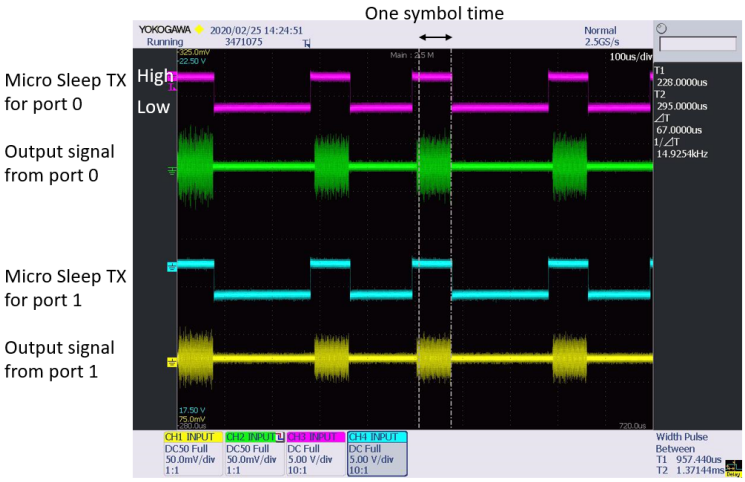

Figure 4.2: Oscilloscope showing signal from antenna ports 0 (top) and 1 (bottom), with only LTE enabled with Micro Sleep TX signal

As seen in Figure 4.2, it is only possible to show two antenna ports and MSTX signals at a time, which means that for a 4TX radio, it will be necessary to look at multiple configurations to be able to investigate the output signals from the antenna ports.

Also seen in Figure 4.2, the MSTX signal can be either high or low. When the signal is high, the PA is supplied with power, and when the signal is low, the power to the PA is cut off. This is utilized as seen in figure 4.2. When the output signal from each port is flat during symbol times, the PA would only waste power being turned on. Therefore, this is also where the MSTX signal is low. There is a short start-up time for the PA though, this can be seen in Figure 4.2 as the MSTX signal is wider than one symbol time, and is set to high a short time before the symbol time starts. Cutting the power takes no time.

The symbols seen from both antenna ports in Figure 4.2 are the CRSs seen in Figure 2.10. Port 0 and 1 will each have 4 symbols transmitted.

By configuring the cell setup, it is possible to view other antenna ports on the oscilloscope. In Figure 4.3, antenna ports 0 and 2 were connected to the oscilloscope. As seen, antenna port 2 will only have 2 CRSs while antenna port 0 has 4. The symbol index for these reference signals are also different. This is in accordance to Figure 2.10.

In Figure 4.3, antenna port 2, the lower signal, has three symbols with MSTX high, while there are only 2 CRSs. In symbol 0, there are other signals transmitted in every subframe, such as the PDCCH, PCFICH, and the PHICH. These will be transmitted on all antenna ports, and therefore the MSTX signal is high during

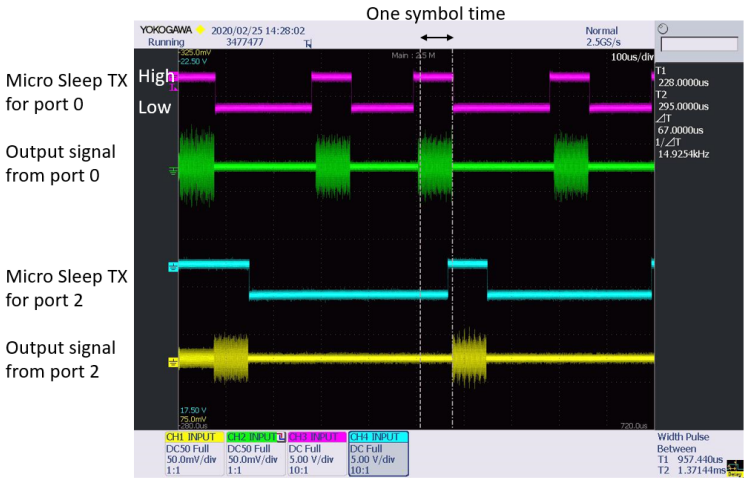

Figure 4.3: Oscilloscope showing signal from antenna ports 0 (top) and 2 (bottom), with only LTE enabled with Micro Sleep TX signal

this symbol time for antenna ports 2 and 3.

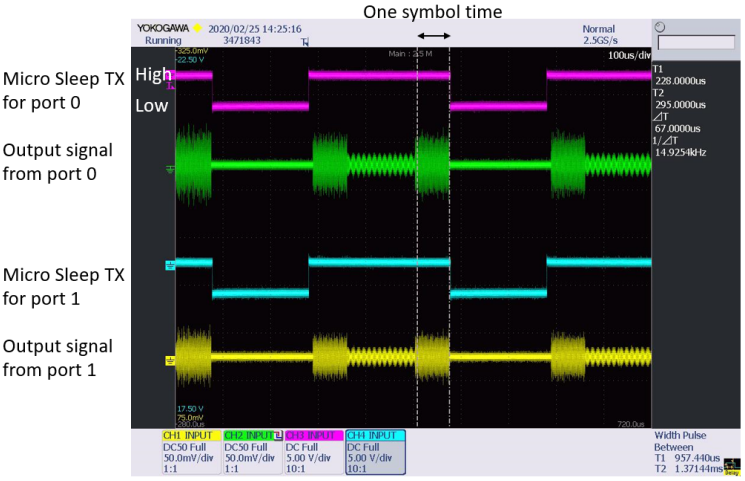

Figure 4.4: Oscilloscope showing signal from antenna ports 0 (top) and 1 (bottom), with LTE and NB-IoT enabled, with Micro Sleep TX signal

Figure 4.4 shows what the signal looks like from antenna ports 0 and 1 when NB-IoT is activated on the cell. Symbol indexes 5, 6, 12, and 13 now carry the NRS. The signal in these symbol slots is narrower as the power is lower due to these signals being transmitted in a single PRB, as compared to over the entire LTE bandwidth in the case of the CRS in symbols 0, 4, 7 and 11.

4.3.2 Power Consumption

A measurement of the power consumption of the RU with and without NB-IoT activated was carried out to find out how much the power consumption increases when NB-IoT is activated.

Table 4.1: Comparison of average power consumption with and without NB-IoT

Without NB-IoT	With NB-IoT	Increase (W)	Increase (%)
123.4 W	144.1 W	20.7 W	16.8 %

As seen in table 4.1, activating NB-IoT causes a 16.8% increase in power consumption, or 20.7 W. NB-IoT in-band uses only one PRB, or 180 kHz of the 10 MHz bandwidth, although this is boosted by using 3 additional PRBs. This would constitute 4 out of 50 PRBs, which is 8%. The next step was then to investigate this increase.

4.3.3 Occupied Symbol Ratio

A script was run for 5 seconds in an LTE cell with zero load, and the resulting log was processed and the average ratio of occupied symbols was calculated for each subframe, as well as each antenna port. This gave the occupied symbols ratios found in table 4.2

Table 4.2: Occupied symbols ratio, zero load without NB-IoT

		Antenna Port				
		0	1	2	3	Average
Subframe	0	0.69	0.69	0.62	0.62	0.65
	1	0.29	0.29	0.21	0.21	0.25
	2	0.29	0.29	0.21	0.21	0.25
	3	0.29	0.29	0.21	0.21	0.25
	4	0.29	0.29	0.21	0.21	0.25
	5	0.72	0.72	0.68	0.68	0.7
	6	0.29	0.29	0.21	0.21	0.25
	7	0.29	0.29	0.21	0.21	0.25
	8	0.29	0.29	0.21	0.21	0.25
	9	0.29	0.29	0.21	0.21	0.25
	Average	0.37	0.37	0.3	0.3	0.34

This occupied symbols ratio should be interpreted as, for instance, antenna port 0, subframe 0, has the ratio 0.69. This means that on average, 69% of the symbols transmitted in this subframe on this antenna port are occupied by data, and therefore the PA has to be powered on at least 69% of the time. For antenna ports 0 and 1, this can be compared to the resource grid in Figure 2.9. As can be

seen, subframes 0 and 5 have a higher average ratio of occupied symbols than the others, due to the scheduling of the signals PBCH, PSS, and SSS.

The same measurement was done for the cell after activating NB-IoT in-band. This gave the occupied symbols ratio seen in table 4.3.

Table 4.3: Occupied symbols ratio, zero load with NB-IoT

		Antenna Port				
		0	1	2	3	Average
Subframe	0	0.88	0.88	0.94	0.94	0.91
	1	0.57	0.57	0.51	0.51	0.54
	2	0.57	0.57	0.51	0.51	0.54
	3	0.57	0.57	0.51	0.51	0.54
	4	0.72	0.72	0.72	0.72	0.72
	5	0.93	0.93	0.97	0.97	0.95
	6	0.57	0.57	0.51	0.51	0.54
	7	0.57	0.57	0.51	0.51	0.54
	8	0.57	0.57	0.51	0.51	0.54
	9	0.72	0.72	0.72	0.72	0.72
	Average	0.67	0.67	0.64	0.64	0.65

These results can be compared to the resource grid of NB-IoT presented in section 2.10. As seen in table 4.3, subframes 0 and 5 will always be very close to fully occupied, even for a zero load, due to the transmission of NPBCH and NPSS respectively. Every other subframe 9 will be occupied by the NSSS. Every other subframe 4 is also occupied by the transmission of the System Information Block (SIB)1-Narrowband (NB) [12, p. 271].

4.3.4 Comparison With and Without NB-IoT

In order to compare a system with NB-IoT and without NB-IoT, table 4.4 below presents both systems' average ratio of occupied symbols, as well as a measurement of the increase in occupied symbols.

Table 4.4: Comparison of average occupied symbol ratio with and without NB-IoT

With NB-IoT	Without NB-IoT	Increase
0.65	0.34	91 %

As seen in table 4.4, activating NB-IoT increases the amount of symbols occupied on average by 91%. This means that almost twice as many symbols are occupied when NB-IoT is activated in-band in an LTE cell. This implies that by activating NB-IoT in a 4TX LTE cell as in-band, MSTX will only be able to power off the PA about half as often as without NB-IoT activated.

Further investigating this at a per antenna port basis, presented below in table 4.5, shows that the increased ratio of occupied symbols differs per antenna port.

Table 4.5: Comparison of average occupied symbol ratio with and without NB-IoT per antenna port

Antenna Port	With NB-IoT	Without NB-IoT	Increase
0	0.67	0.37	81 %
1	0.67	0.37	81 %
2	0.64	0.3	113 %
3	0.64	0.3	113 %

In table 4.5 above, antenna ports 2 and 3 see an increase in occupied symbols of 113%, while antenna port 0 and 1 see an increase of 81%. With NB-IoT activated in-band in a 4TX LTE cell most of the loss in opportunities for MSTX to turn off the PA can be found in antenna port 2 and 3.

4.3.5 Simulation

In order to compare the different transmission schemes, a simulation was created in Matlab. This simulation calculates the Bit Error Ratio (BER) over a range of SNR simulating 10 million QPSK-coded bits transmitted over 500 randomly generated normalized independent and identically distributed Rayleigh channels. Channels are normalized so that all of them have a power which is relative to the average power of all channels. The simulation uses SISO, MISO, and 2x2 Alamouti coding as a comparison to be able to compare the performance of the features implemented to known baselines. By plotting the BER over the SNR, it is possible to visualize array gain and diversity gain. Diversity gain is the slope of the BER curve as the SNR increases. Array gain can be seen as a shift to the left in the curve [21, p. 88]. These concepts are illustrated in Figure 4.5. The formulas used for this simulation are found in [21, p. 93-97].

4.3.6 NB-IoT 4TX

NB-IoT is designed to use one or two logical antenna for transmission. In the case of in-band NB-IoT however, the enclosing LTE cell could be configured to use more than two logical antenna ports. The resource grid for in-band NB-IoT is designed to handle this as explained previously in section 2.10.3. It is then up to the implementation how to handle this situation with more antenna ports in the enclosing LTE cell than the NB-IoT cell [12, p. 232].

Current Implementation

For the case with an RBS where NB-IoT is configured as in-band in an LTE cell configured as using 4 logical antenna ports, the symbols from the two logical antenna ports in the NB-IoT cell are mapped to four logical antenna ports, and subsequently transmitted on four RF-chains. This mapping is carried out using

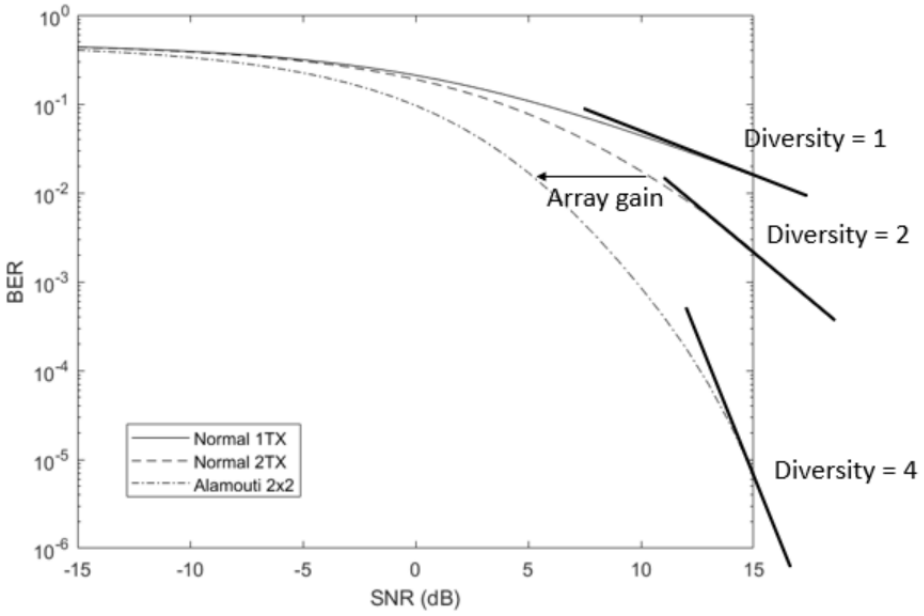

Figure 4.5: BER simulation of SISO, 2x1 MISO Alamouti, and 2x2 MIMO Alamouti

a precoder matrix. Different precoder matrices are used for different DL physical channels [15].

A simulation was run in Matlab to find how this implementation compares to different systems. For reference, a SISO system, with diversity order 1, a 2x1 MISO system with diversity order 2, and a 2x2 MIMO system with diversity order 4, were simulated as well. All but the SISO system use the SFBC scheme previously presented in section 2.10.5 in order to extract diversity gain. This simple simulation assumes that the channel is unknown to the transmitter and as such does not extract any transmit gain. The BER was calculated for different SNRs. The diversity can be found as the slope of the BER curve as the SNR increases.

As seen in Figure 4.6, the slopes for 2x1 MISO, in the figure named Normal 2TX, and for NB-IoT 4TX are almost parallel. This indicates that the diversity order is similar.

4.4 Antenna Port Muting

As uncovered during the investigation, antenna ports 2 and 3 cause the largest increase in occupied symbols ratio, as seen in table 4.5, and with the current implementation, there is no diversity gain from using 4 antenna ports compared to 2 antenna ports. Therefore, a method for muting antenna ports 2 and 3 was implemented.

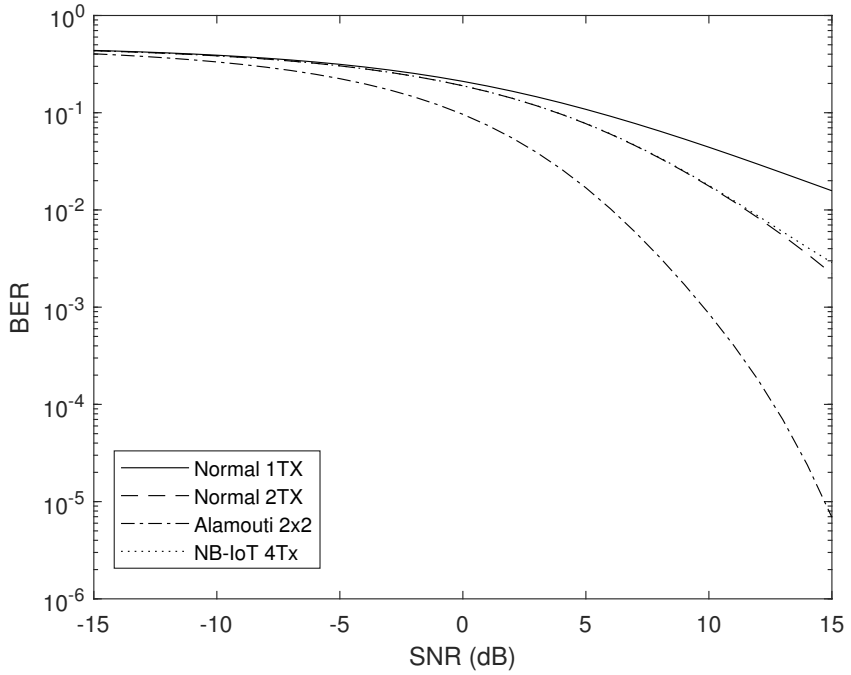

Figure 4.6: BER comparison of NB-IoT 4TX

4.4.1 Proposed Solution

The proposed solution is to enable NB-IoT on antenna ports 0 and 1 only. As NB-IoT is specified as using up to two antenna ports, and the mapping of antenna ports to physical antennas is up to the implementation, this would still adhere to the standard [12, p. 232]. The precoder matrix would now be changed to equation 4.3 for the NB-IoT PRB.

$$\begin{bmatrix} y_0 \\ y_1 \\ y_2 \\ y_3 \end{bmatrix} = \begin{bmatrix} 1 & 0 \\ 0 & 1 \\ 0 & 0 \\ 0 & 0 \end{bmatrix} \begin{bmatrix} x_0 \\ x_1 \end{bmatrix} \tag{4.3}$$

4.4.2 Theoretical Results

Given the new precoder matrix, the ratio of occupied symbols on each antenna port would theoretically be changed to the values presented in table 4.6.

As seen in table 4.6, the average ratio of occupied symbols would change to 0.485 with NB-IoT activated, rather than the 0.65 seen with the current implementation. This constitutes a reduction of the increased ratio of occupied symbols of about 53% ($\frac{0.65-0.485}{0.65-0.34} = 0.532$). This means that MSTX would be able to turn off the PA 53% more often with the proposed solution.

Table 4.6: Theoretical comparison of current implementation and proposed solution with port muting

	Current implementation			Proposed implementation		
Antenna Port	Without NB-IoT	With NB-IoT	Increase	Without NB-IoT	With NB-IoT	Increase
0	0.37	0.67	81 %	0.37	0.67	81 %
1	0.37	0.67	81 %	0.37	0.67	81 %
2	0.3	0.64	113 %	0.3	0.3	0 %
3	0.3	0.64	113 %	0.3	0.3	0 %
Average	0.34	0.65	91 %	0.34	0.485	43 %

If the PA is turned off 53% more of the time with this proposed solution, then an approximation of the power saved by implementing this would be the increase in power consumption seen when activating NB-IoT with this reduction subtracted. As seen in table 4.7, the power consumption increased by 20.7 W on average in a zero load 4TX LTE cell with NB-IoT activated using the current implementation. With the proposed solution, this figure would be lowered to $20.7 \cdot 0.532 = 11W$ which means a decrease in the power consumption to $20.7-11 = 9.7W$ as presented in table 4.7.

Table 4.7: Theoretical comparison of power consumption increase with current and proposed implementation with port muting

Implementation	Without NB-IoT	With NB-IoT	Increase
Current	123.4 W	144.1 W	20.7 W (16.8 %)
Proposed	123.4 W	133.1 W	9.7 W (7.9 %)

4.4.3 Implementation

Occupied Symbol Ratio

The first step was to alter the code so that MSTX worked properly and only turned the PA on for NB-IoT symbols on antenna ports 0 and 1, and not antenna ports 2 and 3. The functionality of this was verified by using the same method as in section 4.3.3. Four measurements were made in total to gather the occupied symbol ratio for each antenna port and with antenna port muting toggled on and off. The results from these measurement are shown in table 4.8.

Symbol Mapping

After verifying that the measured occupied symbol ratio matched the theoretical values, the next step in the implementation was started. As the first step only turned off the PA during NB-IoT symbols on antenna ports 2 and 3, it was now

Table 4.8: Resulting occupied symbol ratio comparison of with and without antenna port muting

	Power save off		Power save on	
Antenna Port	Without NB-IoT	With NB-IoT	Without NB-IoT	With NB-IoT
0	0.37	0.67	0.37	0.67
1	0.37	0.67	0.37	0.67
2	0.3	0.64	0.3	0.3
3	0.3	0.64	0.3	0.3
Average	0.34	0.65	0.34	0.485

necessary to make sure that no NB-IoT symbols were mapped to be transmitted on these antenna ports. If these symbols are not empty, the tail-piece of them will be transmitted because of the width of the MSTX, as explained in section 4.3.1, being wider than one symbol time.

The implementation makes sure that if antenna port muting is turned on, the NB-IoT symbols in the symbol buffer for antenna ports 2 and 3 are filled with zeros. The check for if antenna port muting is turned on or off is based on the same variable as used for the occupied symbol ratio code. This implementation was verified by using the same method as described in section 4.3.1. By looking at the signal in an oscilloscope, it is possible to verify that the correct symbols are empty and that there is no tail-part of symbols transmitted for symbols where the PA has been turned off by MSTX.

Two different configurations were investigated. The first one was with NB-IoT activated and antenna ports 0 and 2 connected to the oscilloscope without antenna muting activated. This is shown in Figure 4.7. Figure 4.8 shows the second configuration with the same antenna ports connected but with antenna port muting activated.

Figure 4.7 shows that in the normal case, the NRS transmitted in symbol indices 5, 6, 12, and 13, are transmitted on both antenna ports. As shown in section 4.3.6, the NB-IoT symbols on antenna port 2 are copies of the NB-IoT symbols transmitted on antenna port 0. Once activating the antenna port muting feature, the MSTX signal is low at the symbol indices where the NRSs were previously found on antenna port 2.

By looking closely at Figure 4.8, the MSTX signal for symbol 0 actually rises already at the end part of symbol 13 for the yellow signal from antenna port 2. If there was an NRS symbol mapped to be transmitted here, as it would be if the antenna port was not muted, there would be a small fragment transmitted in the end of symbol 13. As there is no fragment of a signal there, it can be concluded that the implementation antenna port muting of NB-IoT signals on antenna ports 2 and 3 was completed.

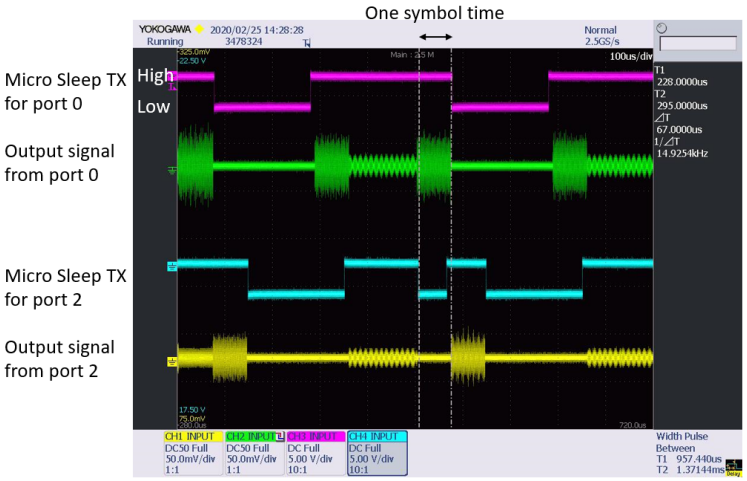

Figure 4.7: Oscilloscope showing signal from antenna ports 0 (top) and 2 (bottom), with LTE and NB-IoT enabled, on antenna ports 0 and 2 with Micro Sleep TX signal

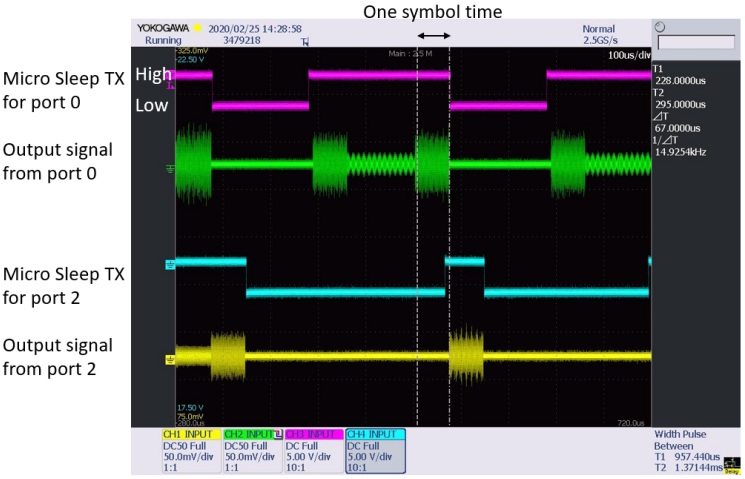

Figure 4.8: Oscilloscope showing signal from antenna ports 0 (top) and 2 (bottom), with LTE and NB-IoT enabled, with Micro Sleep TX signal and NB-IoT muted on antenna ports 2 and 3

Verifying Functionality

In order to verify the functionality of the implementation, a UE was connected to the RBS. First this was done without antenna port muting activated. After verifying that it was possible to attach the UE to the cell and that the desktop computer could ping another computer on the network by using the UE as a modem, antenna port muting was activated. Both attaching and pinging was

successful when the NB-IoT signal was muted on antenna ports 2 and 3.

4.5 Ericsson Confidential

This section has been removed to protect Ericsson confidentiality.

4.6 Downlink Subframe Deactivation (DSD)

DSD is a novel feature that combines declaring specific subframes as invalid with adding new carriers in the NB-IoT to lower power consumption while retaining capacity. While an NB-IoT carrier only occupies a single PRB of the LTE cells bandwidth, it adds multiple new signals in the time-domain on symbol times that were previously left empty in the case of an empty subframe. This means that there are fewer opportunities for MSTX to turn off the PA when NB-IoT is activated in the cell.

As presented previously in section 2.11, LESS attempts to spread data transmissions in the frequency-domain rather than the time-domain by buffering non-critical transmissions until a threshold is reached, or a critical transmission is made. This enables MSTX to trigger more often as there are more instances where the entire frequency-domain is empty so that the PA can be turned off.

This section explores a new way to mimic this effect in NB-IoT without rescheduling transmissions, but by using the SIB1-NB to indicate subframes as invalid, and adding a new carrier.

4.6.1 Proposed Solution

By moving the subframes used for DL data transmissions, such as NPDCCH and NPDSCH to the same subframe indices as the "always on" signals, it is possible to increase the frequency of MSTX. By looking at the occupied symbols ratio in table 4.3, there are a few subframes that regularly see a higher occupied symbols ratio than the rest. These subframes are subframes 0, 4, 5, and 9. These contain what can be referred to as "always on" transmissions. These are the NPBCH, NPSS, NSSS, and the transmission of SIB1-NB over NPDCCH.

Comparing table 4.3 with table 4.2, subframes 0 and 5 see an increased occupied symbol ratio compared to other subframes both with NB-IoT activated and without. Activating NB-IoT increases the occupied symbol ratio for subframes 4 and 9.

An optional field, called DL bitmap, enables declaring specific subframes as invalid DL subframes. By moving all data transfer to subframes 0, 4, 5, and 9, it is possible to reduce the total occupied symbols ratio over all subframes and antenna ports. In order to retain capacity, a new carrier can be opened on another PRB with the same subframes configured as valid DL subframes.

DL Bitmap

The DL bitmap, named DL-bitmap-NB in the technical specification, is an optional field in the SIB1-NB which indicates to the UE which subframes are valid for downlink data transmission [22]. If a subframe is marked as invalid for downlink data transmission, the UE is not to expect any data nor NRS in this subframe [12, p. 239].

Adding Another Carrier

As mentioned in section 2.10.2, there are two carrier types in NB-IoT, the anchor carrier, and the non-anchor carrier. Adding a new non-anchor carrier will not create overhead as it does not transmit NPBCH, NPSS, or NSSS. This is therefore the preferred method of increasing the capacity in NB-IoT in this solution.

4.6.2 Proposed Configuration

Figure 4.9 shows a possible configuration where half of the subframes in a NB-IoT frame are declared as invalid. Another non-anchor carrier is added with the same subframes declared as invalid. The invalid NB-IoT DL subframes can instead be used for normal LTE transmissions. This would result in the same amount of subframes available for NB-IoT DL transmissions. The LTE cell would not lose any additional capacity either, as there is still an equal amount of subframes available for the LTE scheduler.

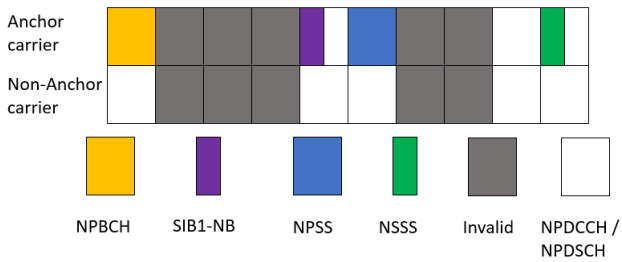

Figure 4.9: Simple illustration of a possible DSD configuration

Using a non-anchor carrier requires that the device has multi-carrier capabilities. This should therefore be dynamic, where a UE without multi-carrier capabilities would be scheduled on the anchor carrier, with a non-anchor carrier added if enough UEs with multi-carrier capabilities are attached to the cell. These UEs would be scheduled on the non-anchor carrier. If more UEs without multi-carrier capacities need to be scheduled, the cell could either dynamically change how many subframes are indicated as invalid, or open up another anchor carrier.

4.6.3 Theoretical Results

By using the measured occupied symbol ratios from tables 4.2 and 4.3, a theoretical occupied symbol ratio can be calculated for the configuration presented in section

4.6.2. The results from this calculation are presented in table 4.9.

Table 4.9: Theoretical occupied symbols ratio, zero load with NB-IoT with DSD configured as shown in section 4.6.2

		Antenna Port				
		0	1	2	3	Average
Subframe	0	0.88	0.88	0.94	0.94	0.91
	1	0.29	0.29	0.21	0.21	0.25
	2	0.29	0.29	0.21	0.21	0.25
	3	0.29	0.29	0.21	0.21	0.25
	4	0.72	0.72	0.72	0.72	0.72
	5	0.93	0.93	0.97	0.97	0.95
	6	0.29	0.29	0.21	0.21	0.25
	7	0.29	0.29	0.21	0.21	0.25
	8	0.57	0.57	0.51	0.51	0.54
	9	0.72	0.72	0.72	0.72	0.72
	Average	0.53	0.53	0.49	0.49	0.51

These theoretical results should be compared to the results in table 4.3 to see the difference in occupied symbol ratio with and without DSD. This comparison is presented in table 4.10.

Table 4.10: Theoretical comparison of average occupied symbol ratio with and without DSD

With NB-IoT	NB-IoT with DSD	Decrease
0.65	0.51	22 %

By using DSD with the configuration described in section 4.6.2, the occupied symbol ratio should theoretically decrease by 22%. To compare NB-IoT with DSD to an LTE cell without NB-IoT, a similar comparison was made to table 4.2, and presented in table 4.11.

Table 4.11: Theoretical comparison of average occupied symbol ratio in an LTE cell and an NB-IoT cell with DSD

Without NB-IoT	NB-IoT with DSD	Increase
0.34	0.51	50 %

Table 4.11 shows that activating NB-IoT in the LTE cell with DSD would increase the average occupied symbol ratio by 50%. Table 4.12 breaks this down per antenna port.

The theoretical power consumption can be calculated by finding how much the increased occupied symbol ratio decreases by activating DSD. This is calculated to be ($\frac{0.65-0.51}{0.65-0.34} = 0.412$) about 41%. This means that the theoretical decrease in

Table 4.12: Comparison of average occupied symbol ratio with and without NB-IoT per antenna port

Antenna Port	With NB-IoT and DSD	Without NB-IoT	Increase
0	0.53	0.37	43 %
1	0.53	0.37	43 %
2	0.49	0.3	63 %
3	0.49	0.3	63 %
Average	0.51	0.34	50 %

the increased power consumption from activating NB-IoT with DSD is ($20.7\ \text{W} \cdot 0.412 = 8.53\ \text{W}$) about 8.5 W. This gives a total power consumption increase of $20.7\ \text{W} - 8.5\ \text{W} = 12.2\ \text{W}$ shown in table 4.13.

Table 4.13: Theoretical comparison of power consumption increase between current implementation and DSD

	Without NB-IoT	With NB-IoT	Increase
Current	123.4 W	144.1 W	20.7 W (16.8 %)
With DSD	123.4 W	135.6 W	12.2 W (9.9 %)

4.6.4 Proposed Implementation

Investigation into how to implement DSD was not done in this thesis.

4.7 Minimizing Power Consumption

A benefit of DSD is that it can be combined with antenna port muting. In this section, a theoretical system will be presented, which aims at lowering the power consumption as much as possible. This will be done by combining DSD with antenna port muting from 4TX to 2TX.

By starting from the occupied symbol ratio from table 4.6, and combining this with the theoretical occupied symbol ratio given by using DSD from table 4.9, the average occupied symbol ratio for the new system combining both will be as shown in table 4.14.

As the average occupied symbol ratio without NB-IoT is 0.34, and with NB-IoT is 0.65, the increase in power consumption from combining antenna port muting and DSD can be calculated in the same way as before. The decreased increase in occupied symbol ratio can be calculated to be ($\frac{0.65-0.42}{0.65-0.34} = 0.742$) about 74%. This gives that the power consumption increase of 20.7 W from activating NB-IoT can be decreased by 74%, or ($20.7\ \text{W} \cdot 0.742 = 15.36\ \text{W}$) about 15.4 W. The power increase would then amount to $20.7 - 15.4 = 5.3$ W. With a comparison shown in table 4.15

Table 4.14: Theoretical occupied symbol ratios with antenna port muting and DSD

	Antenna port 0	Antenna port 1	Antenna port 2	Antenna port 3	Total
4TX to 2TX Muting combined with DSD	0.53	0.53	0.3	0.3	0.42

Table 4.15: Theoretical comparison of power consumption increase between current implementation and antenna port muting combined with DSD

	Without NB-IoT	With NB-IoT	Increase
Current	123.4 W	144.1 W	20.7 W (16.8 %)
Antenna port muting combined with DSD	123.4 W	128.7 W	5.3 W (4.3 %)

Chapter 5
Results

Antenna port muting was implemented in the baseband software and tested on an RBS in the lab. Measurements on occupied symbol ratio and power consumption were made, and a UE was attached to the cell to verify connectivity and measure the impact on the received signal power. In this chapter, these results are presented. The calculations for DSD will be based on the theoretical results.

5.1 Antenna Port Muting

Antenna port muting was implemented in the baseband source code and a variable was added which could be used to toggle the feature on and off through direct memory access. The functionality of the new software was verified by attaching a UE to the RBS and attempting to ping another computer in the lab. If this was successful, the RSRP reported by QXDM was noted. The signal power measurements from QXDM showed that the RSRP decreased by almost 3 dB after activating antenna port muting.

5.1.1 Power Consumption

The power consumption measurements were carried out as previously described in section 4.1.1. Results from these measurements were compared to previous measurements carried out in section 4.3.2. The results are presented in table 5.1.

By muting NB-IoT symbols on antenna ports 2 and 3, an idle LTE cell with NB-IoT activated will see a 8.3% increase in power consumption, as compared to 16.8% for the same cell without antenna port muting.

By using the model presented in section 4.2, it is possible to calculate the total savings in the example network given. Section 3 shows that the average traffic over all different cells in the networks vary greatly, however, a majority of them see next to no traffic on average. For this calculation it will therefore be assumed that the antenna port muting feature operates at 60% efficiency.

Table 5.1: Results from power consumption measurements for antenna port muting

	Average power consumption	Increase compared to default without NB-IoT	Savings compared to default with NB-IoT
Default 4TX Without NB-IoT	123.4 W	-	-
Default 4TX With NB-IoT	144.1 W	20.7 W (16.8 %)	-
4TX to 2TX Muting port 2 and 3	133.7 W	10.3 W (8.3 %)	10.4 W (50.2 %)

The total decrease in energy consumption is given by

$$10.4\text{W} \cdot 24 \cdot 365 \cdot 3 \cdot 100000 \cdot 0.6 \approx 16.4 \text{ GWh} \tag{5.1}$$

This would equal a decreased OPEX given by

$$\frac{10.4}{1000} \text{ kW} \cdot 24 \cdot 365 \cdot 3 \cdot 100000 \cdot 0.6 \cdot \text{US\$0.1029} \approx \text{US\$1.7 million} \tag{5.2}$$

In terms of lowered emissions, the decrease in CO_2 emitted from power production can be given by

$$\frac{10.4}{1000} \text{ kW} \cdot 24 \cdot 365 \cdot 3 \cdot 100000 \cdot 0.6 \cdot 0.449 \text{ kg} \approx 7.4 \text{ kilotons of } CO_2 \tag{5.3}$$

The lowered emissions can be compared to the average carbon footprint of a typical US household of 48 tons of CO_2-equivalents as presented in section 4.2.2. The lowered emissions from using antenna port muting is given by

$$\frac{7400}{48} \approx 154 \text{ average US households} \tag{5.4}$$

5.2 Ericsson Confidential

This section has been removed to protect Ericsson confidentiality.

5.3 DSD

As no implementation was made for DSD, the theoretical results from section 4.6.3 will be used to calculate the energy savings. The theoretical power consumption was presented in table 4.13. Using the same energy model as for antenna port muting, this gives the theoretical savings from using DSD to lower the power consumption increase by 8.5 W presented in table 5.2.

Table 5.2: Savings from DSD according to energy model

	Savings			
	GWh	Million US$	Kiloton CO_2	US households
With DSD	13.4	1.4	6	125

5.4 Minimizing Power Consumption

Section 4.7 showed that it is theoretically possible to reduce the power consumption by about 15.4 W by combining antenna port muting from 4TX to 2TX with the new feature DSD proposed in section 4.6. By using the same energy model as previously, the resulting savings were calculated and are presented in table 5.3.

Table 5.3: Savings from combining antenna port muting and DSD according to energy model

	Savings			
	GWh	Million US$	Kiloton CO_2	US households
4TX to 2TX Muting and DSD	24.3	2.5	10.9	227

5.5 Overview of Energy Savings

All of the energy savings can be compiled into one table to provide an overview of the results from the different features. Table 5.4 contains this overview.

Table 5.4: Overview of energy savings

	Savings			
	GWh	Million US$	Kiloton CO_2	US households
4TX to 2TX Muting ports 2 and 3	16.4	1.7	7.4	154
4TX with DSD	13.4	1.4	6	125
4TX to 2TX Muting and DSD	24.3	2.5	10.9	227

Chapter 6
Discussion and Conclusion

In this chapter the different features presented in this thesis, as well as the energy model, are discussed, together with the future work possible. The chapter finishes with a conclusion of the entire thesis.

6.1 Antenna Port Muting

The results shown in table 5.1 closely match the theoretical results calculated in section 4.4.2 with only a difference of 0.6 W in theoretical power consumption compared to the measured power consumption. This means that looking at changes in occupied symbol ratio is a good way of identifying changes in power consumption.

Implementing antenna port muting is not very invasive and is able to provide substantial savings in an example network in the USA. The RSRP did decrease by 3 dB but it is not clear what consequences this would have in a live network.

One could argue that NB-IoT was designed for 2 antennas with the capability to support an MCL of 164 dB. Using 4 antennas could, in the best case, increase this to an MCL of 167 dB, but this should be seen as a bonus. An NB-IoT network should be planned with an MCL of 164 dB, and therefore using antenna port muting should not negatively affect the coverage. Further, due to NB-IoT using very cheap devices with only a single antenna, it might already be restricted by poor uplink.

To continue with this feature, it would be necessary to try antenna port muting in a live network. This would show the effects on coverage more clearly than the RBS in the lab environment where the UE is connected to the RBS via cable. By measuring the number of connected users over a period of time with and without antenna port muting, it should be possible to come to a conclusion on the effects on cell coverage.

6.2 Ericsson Confidential

This section has been removed to protect Ericsson confidentiality.

6.3 DSD

DSD is a concept that was not fully investigated in this thesis. The theory shows promising results, especially when combining it with antenna port muting. In unison, these two features can theoretically lower the increased power consumption of NB-IoT by 74%.

There are however, a lot of question marks still left regarding DSD. As a non-anchor carrier is not expected to be boosted in the same way as an anchor carrier, this must be solved to ensure the support of an MCL of 164 dB. Another issue is how to handle devices that do not have multi-carrier support.

Further research could be done into possibilities to dynamically adjust the DSD configuration depending on traffic, as well as investigating the possibilities of using more anchor-carriers instead of non-anchor carriers.

6.4 Energy Model

The energy model is very simple and only provides an idea of the energy savings possible. It should be properly investigated how effective the features would be in a live network rather than using the 60% assumption. Further, the radio used in the RBS set up in the lab environment has a low output power of 20 W. It would be interesting to investigate the effects on power consumption the features have on a different radio with a higher output power. Additionally, it should be investigated how these features would work on an NB-IoT network operating as stand-alone or guardband.

6.5 Conclusion

The objective of this thesis was to identify the reasons for the unjustifiable power consumption increase when activating NB-IoT in-band in an LTE cell, and identifying, implementing, and testing new solutions seeking to lower this power consumption.

Research shows that the PA consumes the most power in an RBS and that most of the time, there is no data transmitted in the network. This means that the most effective way of lowering power consumption is by lowering it when the cell is idle. Investigations into NB-IoT signaling found that in an idle cell, the PA was active almost twice as often after activating NB-IoT in the cell.

These insights gained in network characteristics and RBS power consumption lead to the creation of two new power saving features for NB-IoT. One of these features, antenna port muting, was fully implemented in the baseband code, and verified in the lab environment. The second one, DSD, was not implemented, but theoretical calculations showed promising results.

The first feature, antenna port muting, is a feature where antenna ports 2 and 3 are muted. Measurements showed that this lowered the increased power consumption from NB-IoT in the RU by 50.2%, while the RSRP decreased by 3 dB.

A second feature, DSD, which utilizes multiple carriers in conjunction with a bitmap in the SIB1-NB to declare subframes as invalid, was shown to theoretically be able to reduce the increased power consumption by 41%. What showed the most promise was combining antenna port muting with DSD, which was shown to enable a reduction in increased power consumption by 74%.

In conclusion, the NB-IoT standard introduced multiple new signals that came in conflict with already existing power saving features in Ericsson RBSs. In lieu of being able to change the standard, to ensure that NB-IoT signals are transmitted in a more energy efficient way, this thesis presents two solutions seeking to mitigate the consequences of this. With energy efficiency becoming more important in today's environmentally conscious society, it is crucial that future standards are designed to lower the power consumption of idle cells by removing or intelligently planning "always on" signals. Further, it is crucial that add-on features, such as NB-IoT, are designed to work around existing power-saving features. The focus when designing NB-IoT was on minimizing the power consumption in the UE, and a lot of research was conducted in this area, but as shown in this thesis, good reasons exist to reduce the power consumption in the RBS. If a technology like NB-IoT is introduced in 5G, it could make the energy efficiency promised an impossibility.

References

[1] Ericsson, *Ericsson Mobility Report*, November, 2019. Accessed on: February 26, 2020. [Online]. Availabe: https://www.ericsson.com/4acd7e/assets/local/mobility-report/documents/2019/emr-november-2019.pdf

[2] J. Malmodin and D. Lundén, *The electricity consumption and operational carbon emissions of ICT network operators 2010-2015*, Stockholm, 2018. Accessed on: March 27, 2020. [Online]. Available: http://www.diva-portal.org/smash/record.jsf?pid=diva23A1177210

[3] GSMA, *Energy Efficiency: An Overview*. Accessed on: March 9, 2020. [Online]. Available: https://www.gsma.com/futurenetworks/wiki/energy-efficiency-2/

[4] M. Muntean, D. Guizzardi, E. Schaaf, M. Crippa, E. Solazzo, J. Olivier, E. Vignati, "Fossil CO2 emissions of all world countries - 2018 Report". Publications Office of the European Union, 2018. Accessed on: April 23m 2020. [Online]. Available doi: 10.2760/30158

[5] E. Dahlman, S. Parkvall, J. Sköld, *4G, LTE-Advanced Pro and The Road to 5G*, 3rd ed. London: Elsevier, 2016.

[6] E. Dahlman, S. Parkvall, J. Sköld, *5G NR: The Next Generation Wireless Access Technology*. London: Elsevier, 2018.

[7] GSMA, *NB-IoT Deployment Guide to Basic Feature set Requirements*, June, 2019. Accessed on: March 9, 2020. [Online]. Available: https://www.gsma.com/iot/wp-content/uploads/2019/07/201906-GSMA-NB-IoT-Deployment-Guide-v3.pdf

[8] TeleSystem Innovations, *LTE in a Nutshell: The Physical Layer*, 2010. Accessed on: March 9, 2020. [Online]. Available: https://home.zhaw.ch/kunr/NTM1/literatur/LTE%20in%20a%20Nutshell%20-%20Physical%20Layer.pdf

[9] G. Lindell, *An introduction to OFDM Lecture notes in the course Digital communications, advanced course (ETTN01)*. November, 2016. Accessed on: March 9, 2020. [Online]. Available: https://www.eit.lth.se/fileadmin/eit/courses/ettn01/HT2-2017_Rusek/OFDM_lecture_notes_161115.pdf

[10] A. F. Molisch, *Wireless Communications*, 2nd ed. Chichester, United Kingdom: John Wiley & Sons, 2011.

[11] Frame Structure - Downlink. Accessed on: March 25, 2020. [Online]. Available: https://www.sharetechnote.com/html/FrameStructure_DL.html

[12] O. Liberg, M. Sundberg, Y.-P. E. Wang, J. Bergman, J. Sachs, *Cellular Internet of Things Technologies, Standards and Performance*. London: Elsevier, 2018.

[13] Ericsson internal

[14] M. Alsharif, K. Jeong, K. Jin, "Green and Sustainable Cellular Base Stations: An Overview and Future Research Directions", *Energies*, vol. 10, pp. 586, 2017. Accessed on: March 26, 2020. [Online]. Available doi: 10.3390/en10050587.

[15] Ericsson internal

[16] LTE-NB : Frame Structure : Downlink. Accessed on: February 26, 2020. [Online]. Available: https://www.sharetechnote.com/html/Handbook_LTE_NB_FrameStructure_DL.html

[17] Ericsson, *Breaking the energy curve An innovative approach to reducing mobile network energy use*, 2020. Accessed on: March 13, 2020. [Online]. Available: https://www.ericsson.com/493e7e/assets/local/about-ericsson/sustainability-and-corporate-responsibility/documents/2020/breaking-the-energy-curve-report.pdf

[18] U.S. Energy Information Administration, *Electric Power Monthly*, January, 2020. Accessed on: March 31, 2020. [Online]. Available: https://www.eia.gov/electricity/monthly/epm_table_grapher.php?t=epmt_5_6_a

[19] U.S. Energy Information Administration, *Frequently Asked Questions*, February, 2020. Accessed on: March 31, 2020. [Online]. Available: https://www.eia.gov/tools/faqs/faq.php?id=74\&t=11

[20] Center for Sustainable Systems, University of Michigan, *Carbon Footprint Factsheet*, 2019. Accessed on: April 13, 2020. [Online]. Available: http://css.umich.edu/factsheets/carbon-footprint-factsheet

[21] A. Paulraj, R. Nabar, D. Gore, *Introduction to Space-Time Wireless Communications*. New York: Cambridge University Press, 2008.

[22] Third Generation Partnership Project, *Technical Specification 36.331 v15.7.0, Technical Specification Group Radio Access Network, Evolved Universal Terrestrial Radio Access (E-UTRA), Radio Resource Control (RRC), Protocol specification, (Release 15)*, 2019.

Printed by Tryckeriet i E-huset, Lund 2020

LUND
UNIVERSITY

Series of Master's theses
Department of Electrical and Information Technology
LU/LTH-EIT 2020-762
http://www.eit.lth.se